

## Supplementary data

### Synthesis, evaluation of cytotoxicity and molecular docking studies of the 7-acetamide-substituted 2-aryl-5-bromo-3-trifluoroacetylindoles as potential inhibitors of tubulin polymerisation

M.J. Mphahlele, N. Parbhoo

**Figure S1:**  $^1\text{H}$ - and  $^{13}\text{C}$ -NMR spectra of compounds **2a-d**, **3a-d**, **4a-d** and **5a-h**

**Figure S2:** Cytotoxicity of compounds **2a-d**, **4a-d** and **5a-h** against A549 and HeLa cells

**Figure S3:** Dose response curves for **5e-h** against the A549 and HeLa cells

**Figure S4:** Spread sheet for statistical analysis which contains p values for each test

**Figure S5:** Excel spreadsheets for raw data and SD values for compounds **5e-h** as well as GraphPad Prism files for  $\text{IC}_{50}$  determination

Figure S1:  $^1\text{H}$ - and  $^{13}\text{C}$ -NMR spectra of compounds 2a–d, 3a–d, 4a–d and 5a–h

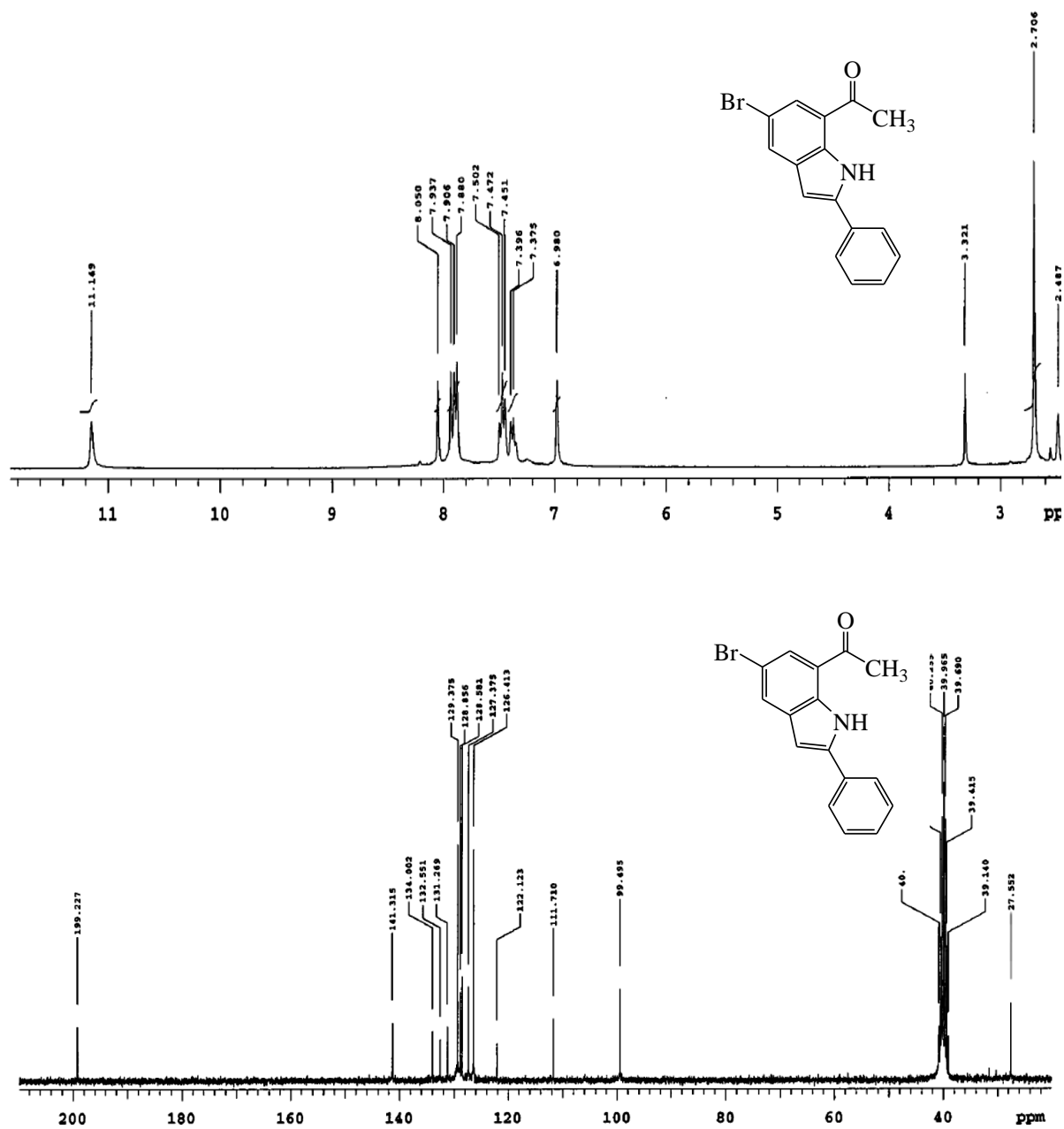


Figure S1.1:  $^1\text{H}$ - and  $^{13}\text{C}$ -NMR spectra of 2a in  $\text{DMSO-}d_6$  at 300 MHz and 75 MHz, respectively.

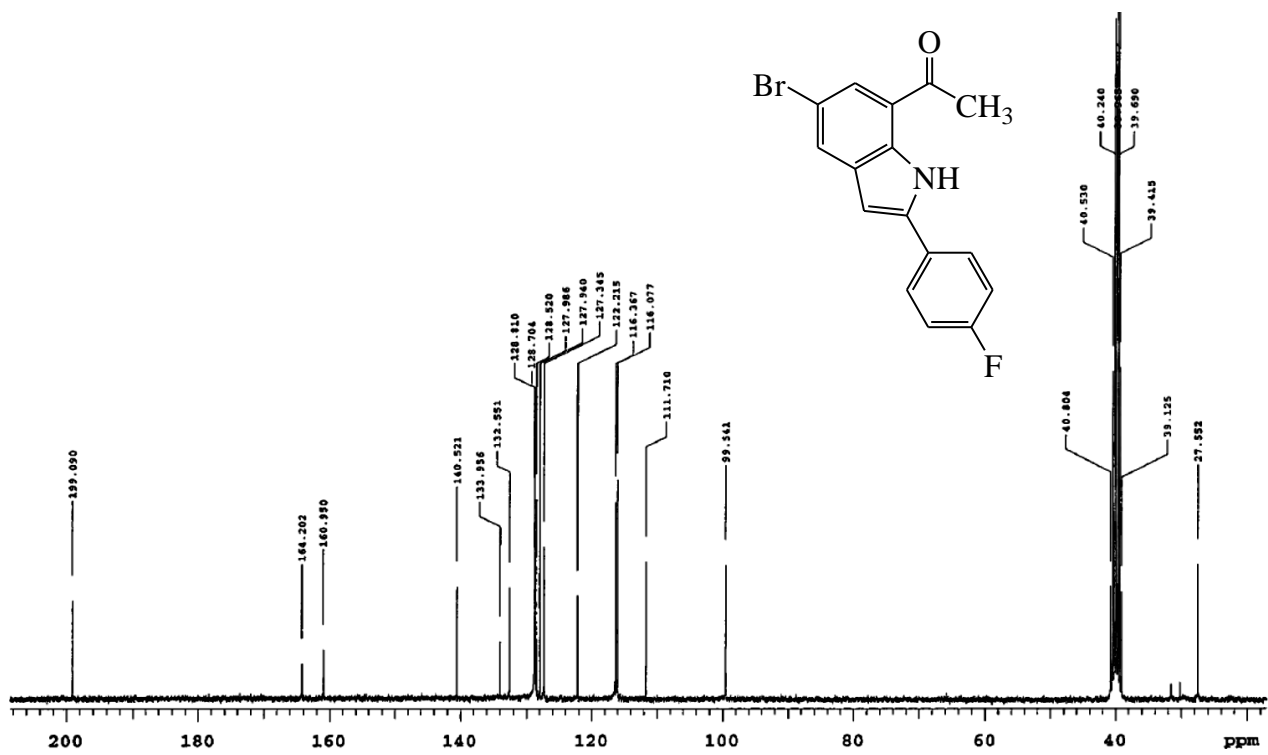
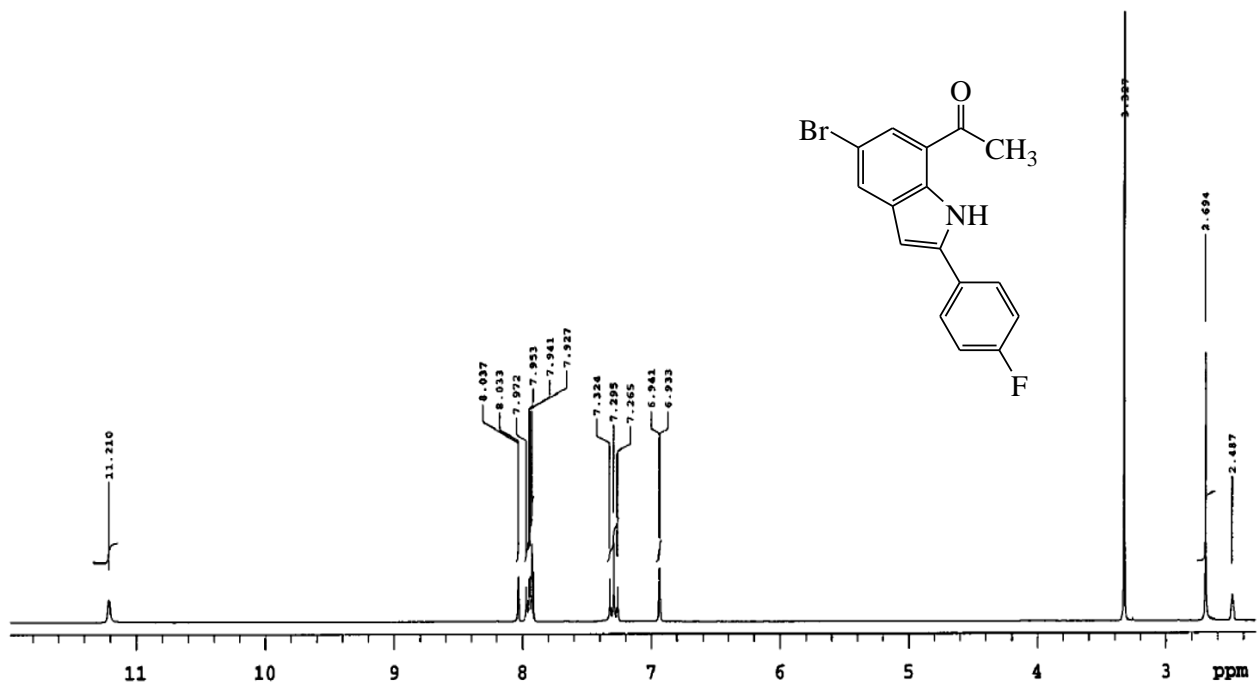


Figure S1.2: <sup>1</sup>H- and <sup>13</sup>C-NMR spectra of **2b** in DMSO-*d*<sub>6</sub> at 300 MHz and 75 MHz, respectively.

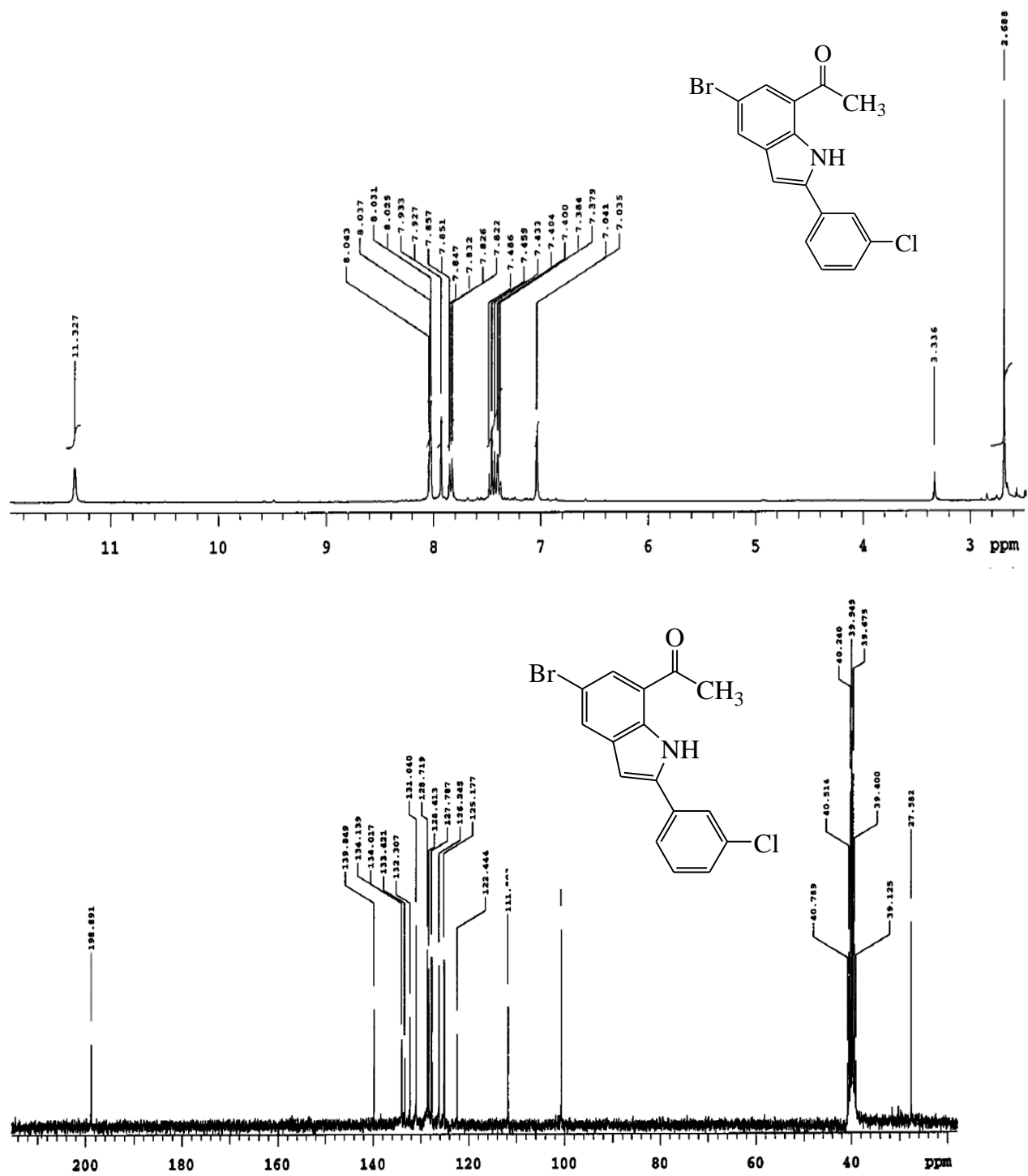


Figure S1.3: <sup>1</sup>H- and <sup>13</sup>C-NMR spectra of 2c in DMSO-*d*<sub>6</sub> at 300 MHz and 75 MHz, respectively.

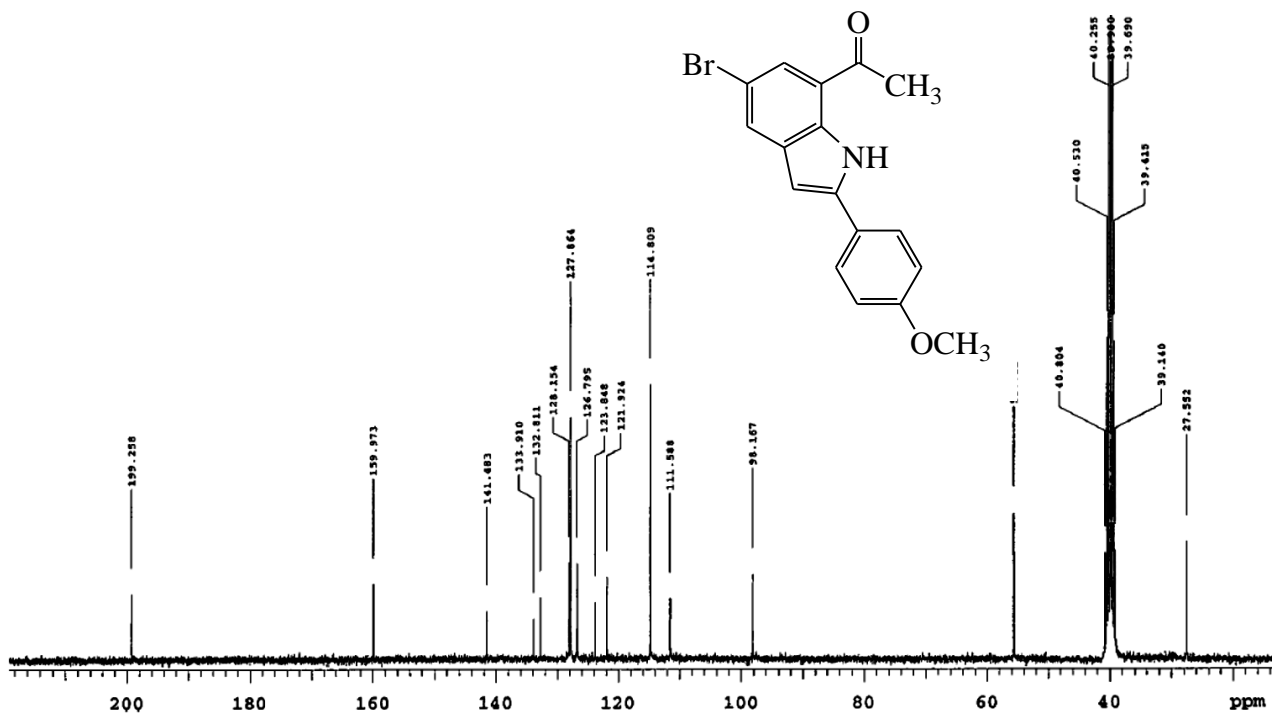
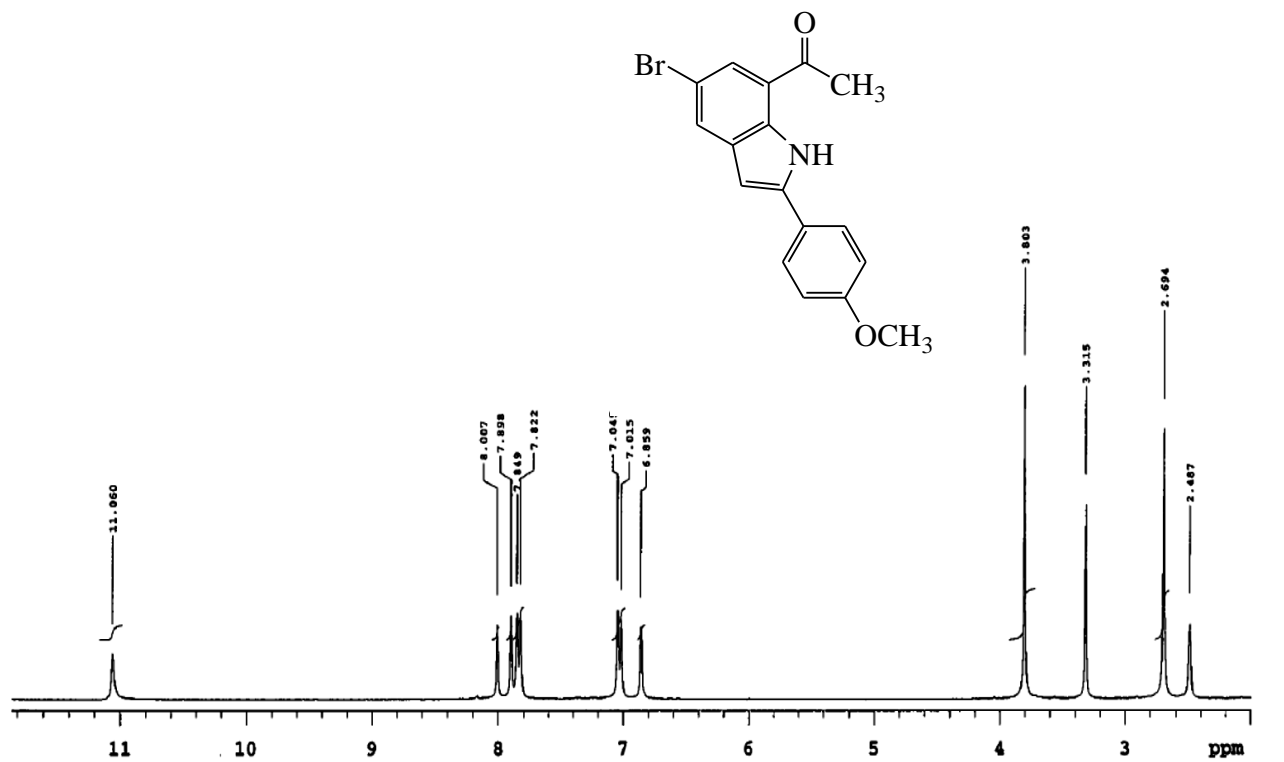


Figure S14: <sup>1</sup>H- and <sup>13</sup>C-NMR spectra of 2d in DMSO-*d*<sub>6</sub> at 300 MHz and 75 MHz, respectively.

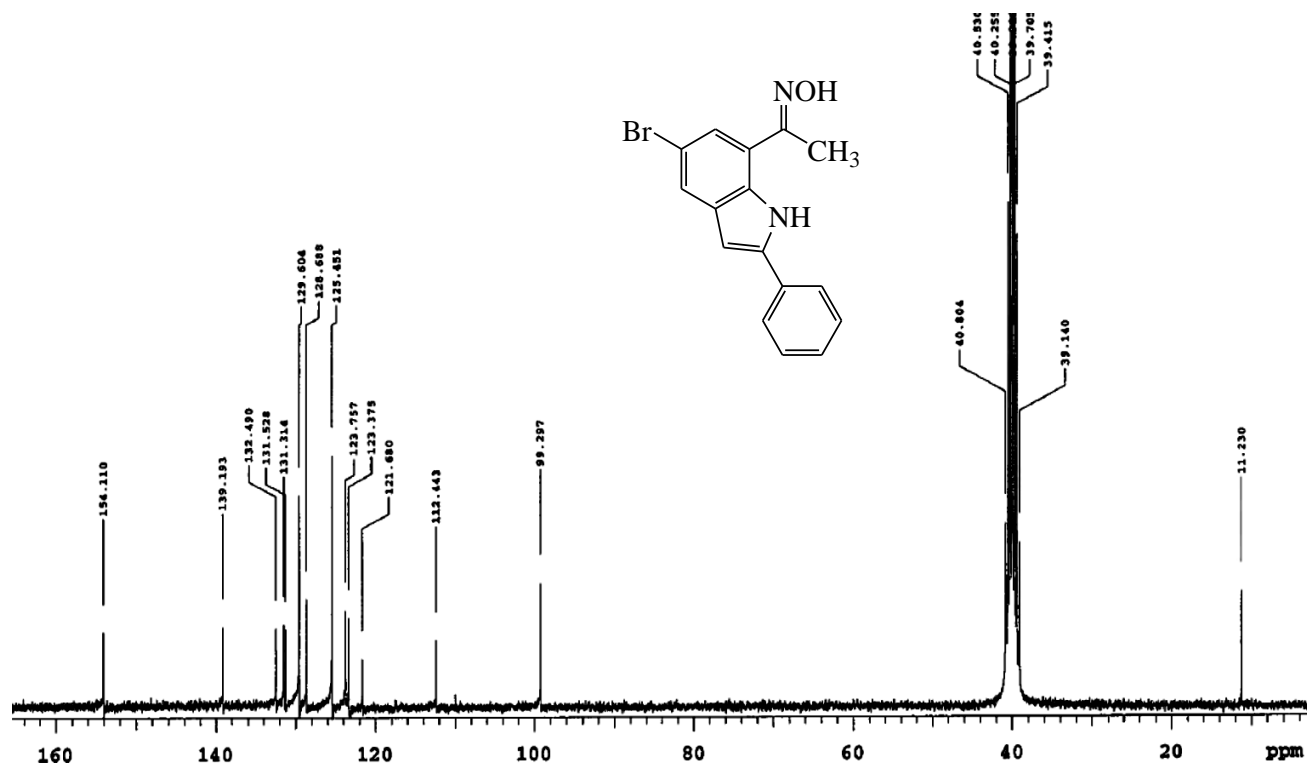
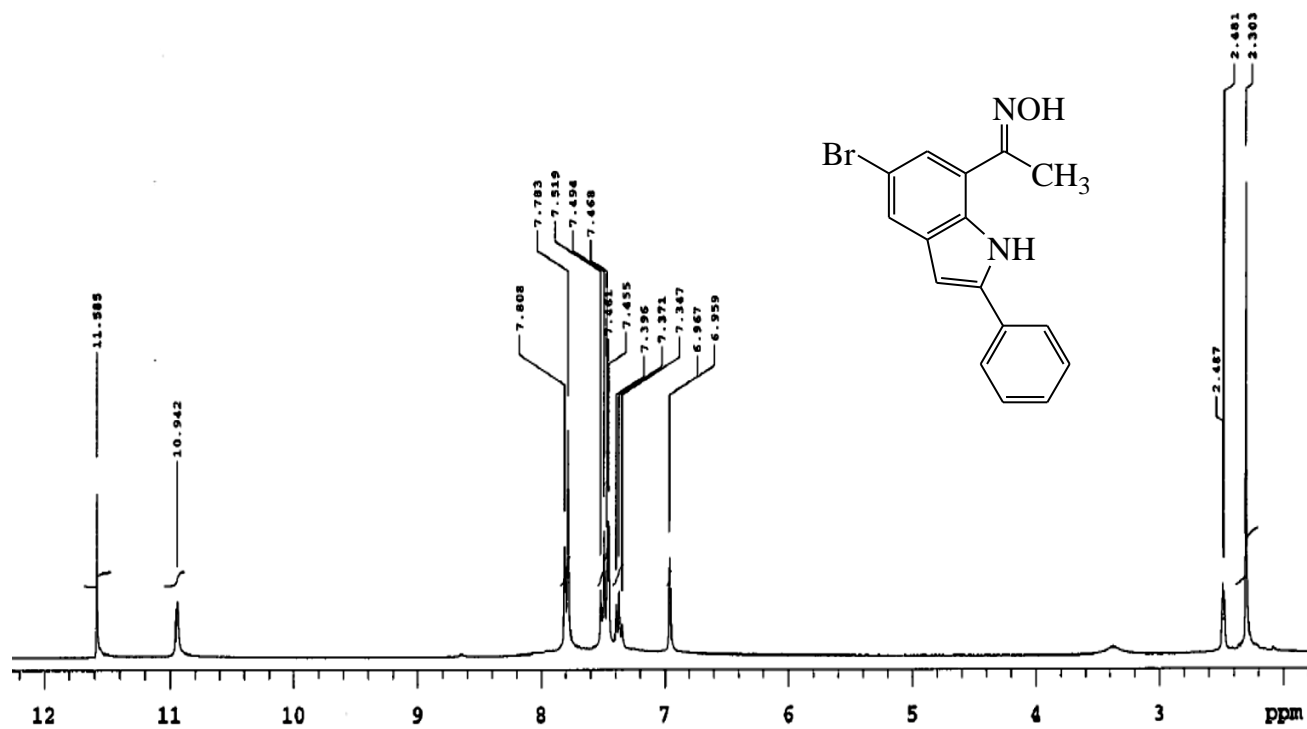


Figure S1.5:  $^1\text{H-}$  and  $^{13}\text{C-NMR}$  spectra of 3a in  $\text{DMSO-}d_6$  at 300 MHz and 75 MHz, respectively.

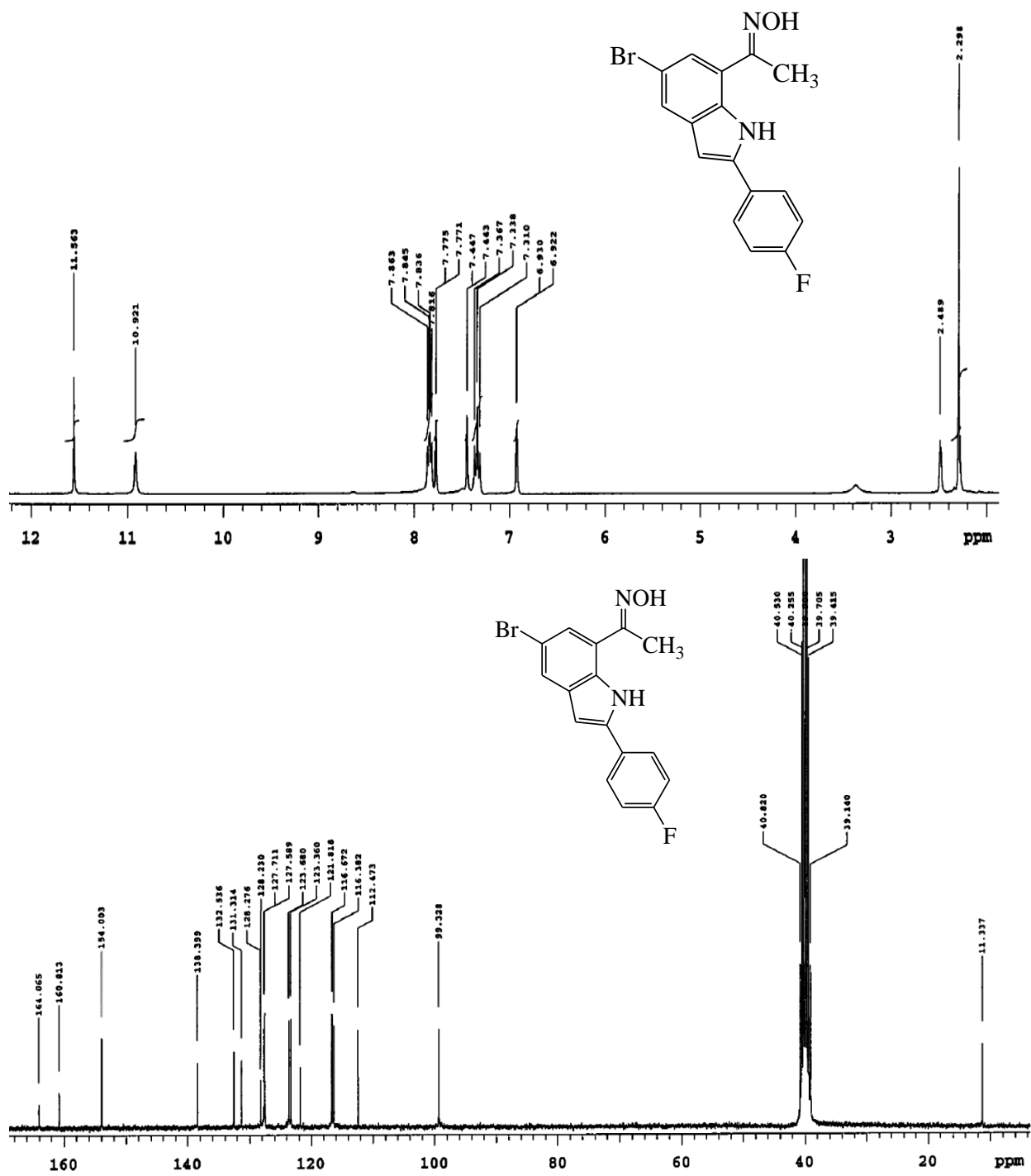


Figure S1.6: <sup>1</sup>H- and <sup>13</sup>C-NMR spectra of **3b** in DMSO-*d*<sub>6</sub> at 300 MHz and 75 MHz, respectively.

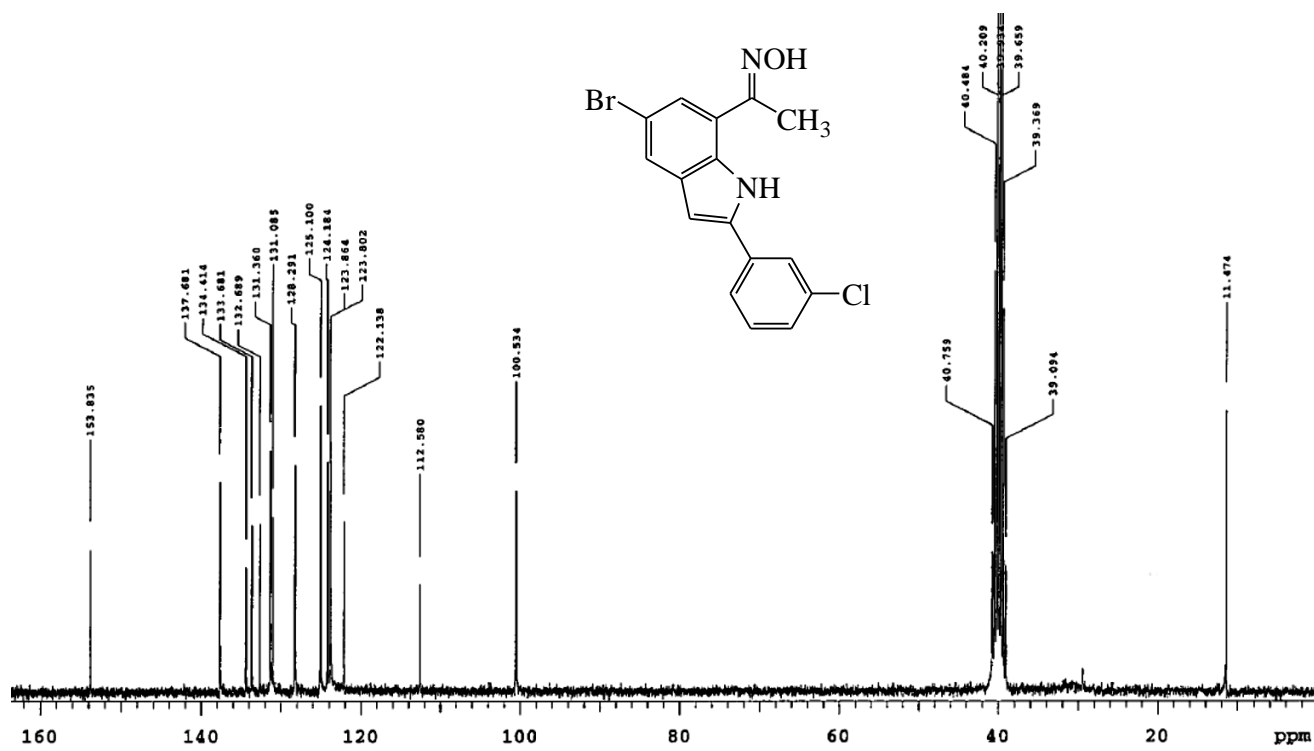
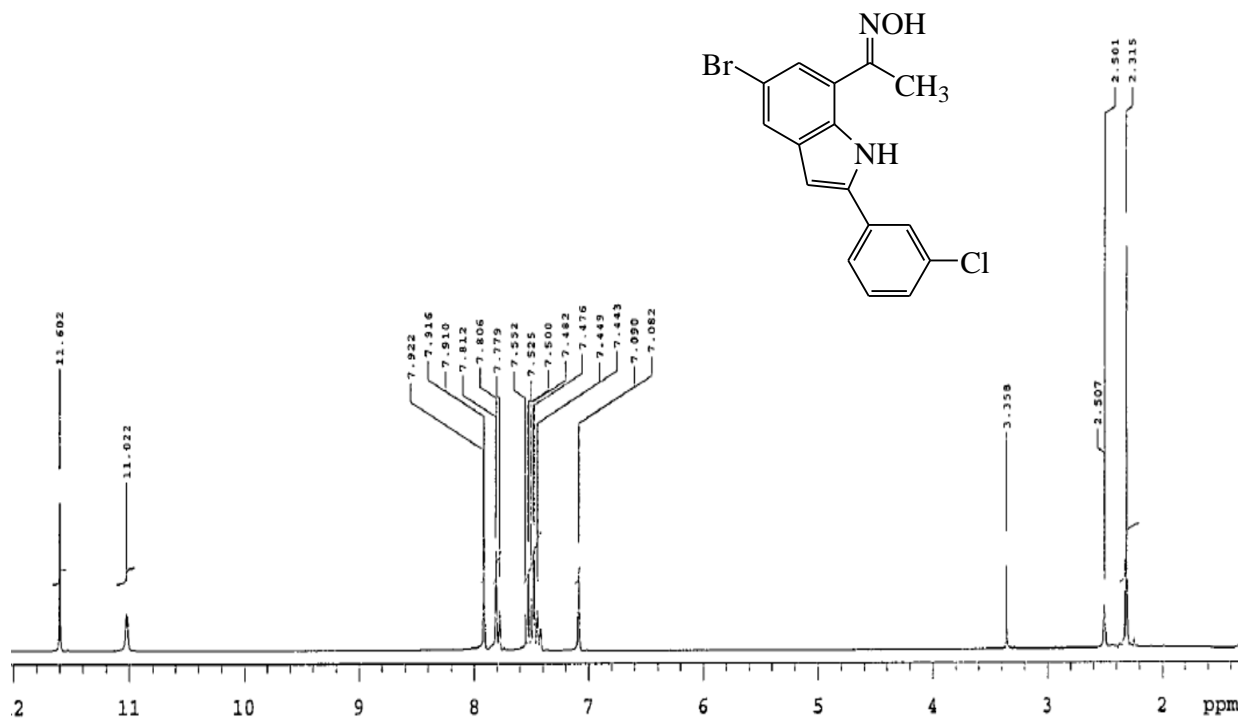


Figure S1.7: <sup>1</sup>H- and <sup>13</sup>C-NMR spectra of 3c in DMSO-*d*<sub>6</sub> at 300 MHz and 75 MHz, respectively.



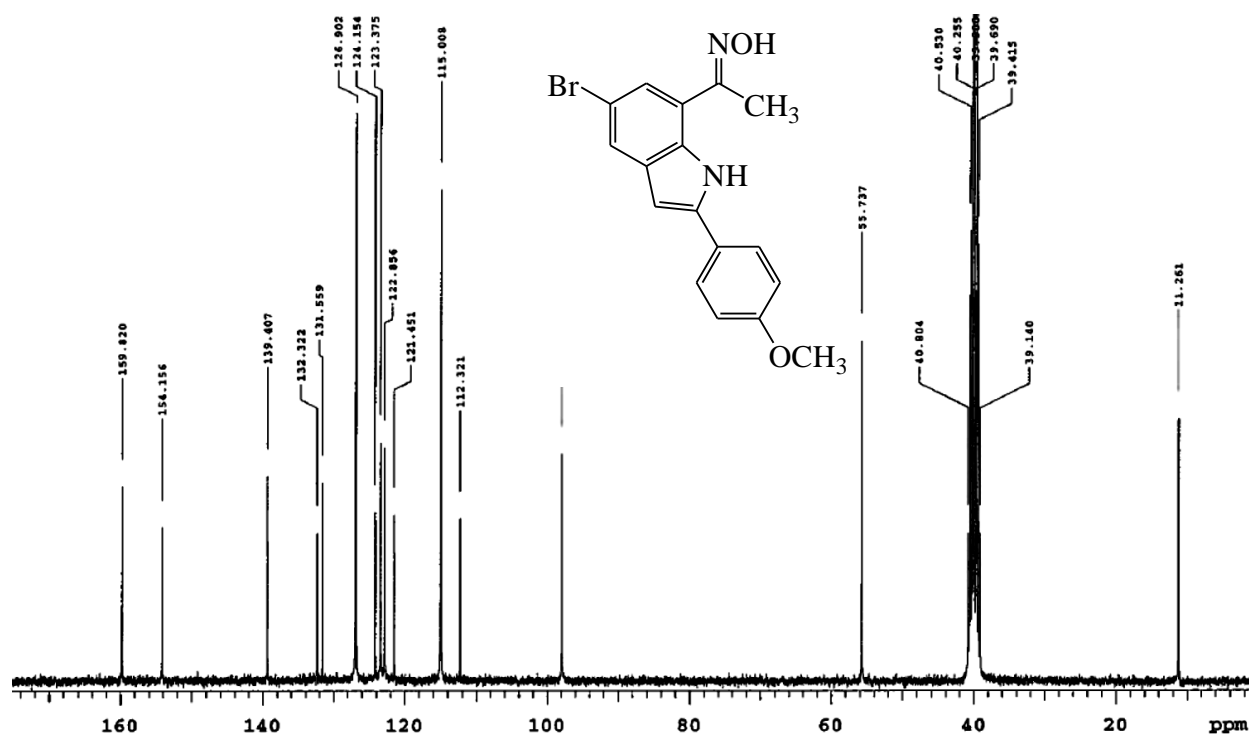
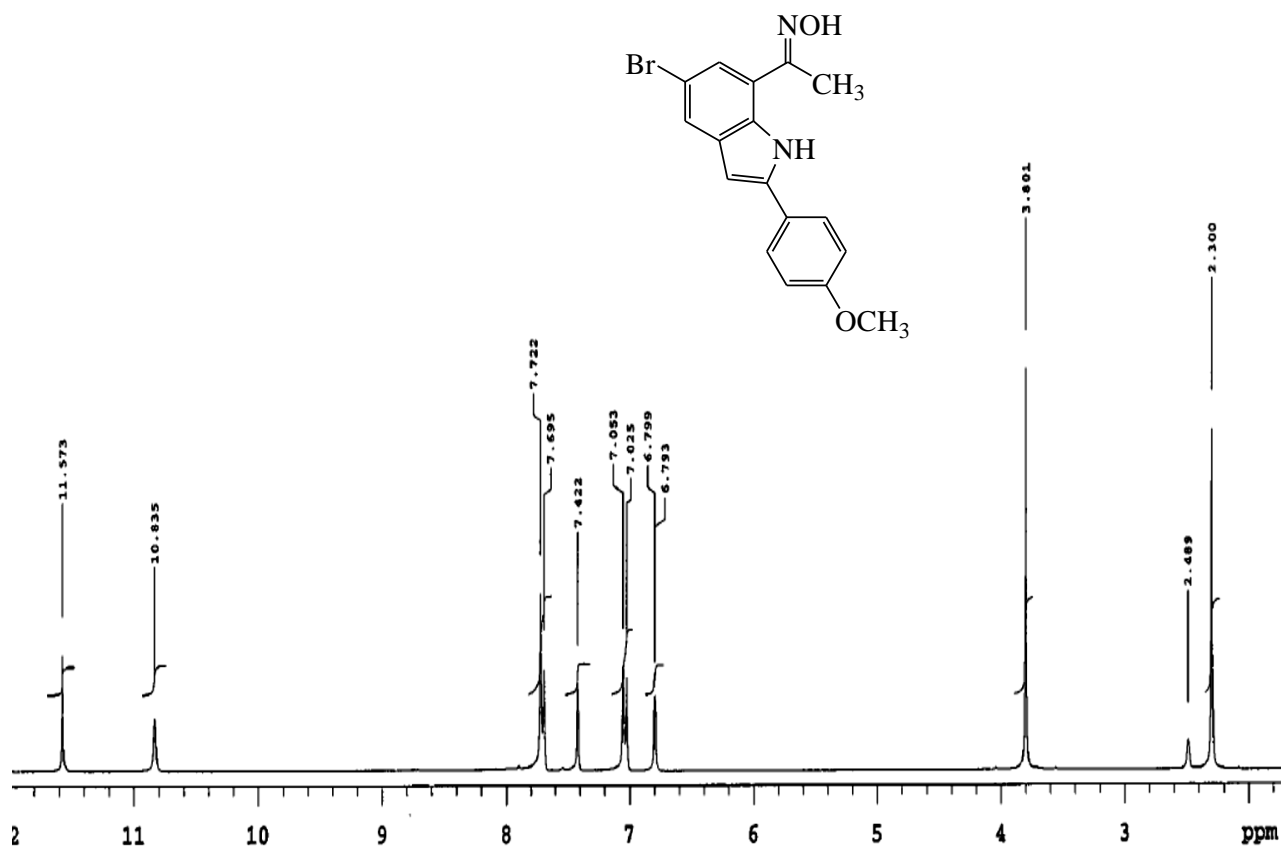


Figure S18: <sup>1</sup>H- and <sup>13</sup>C-NMR spectra of 3d in DMSO-*d*<sub>6</sub> at 300 MHz and 75 MHz, respectively.

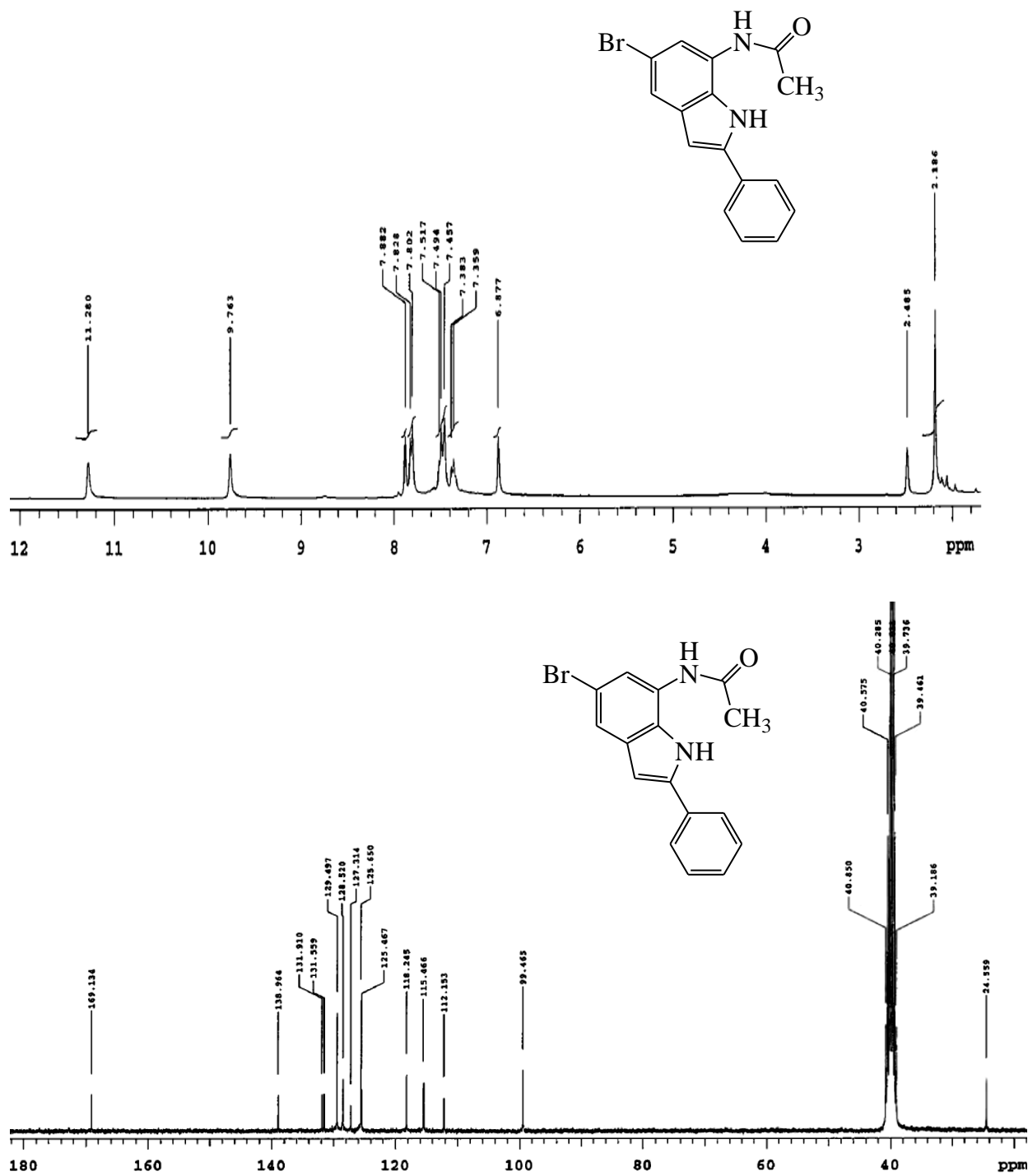


Figure S1.9: <sup>1</sup>H- and <sup>13</sup>C-NMR spectra of 4a in DMSO-*d*<sub>6</sub> at 300 MHz and 75 MHz, respectively.

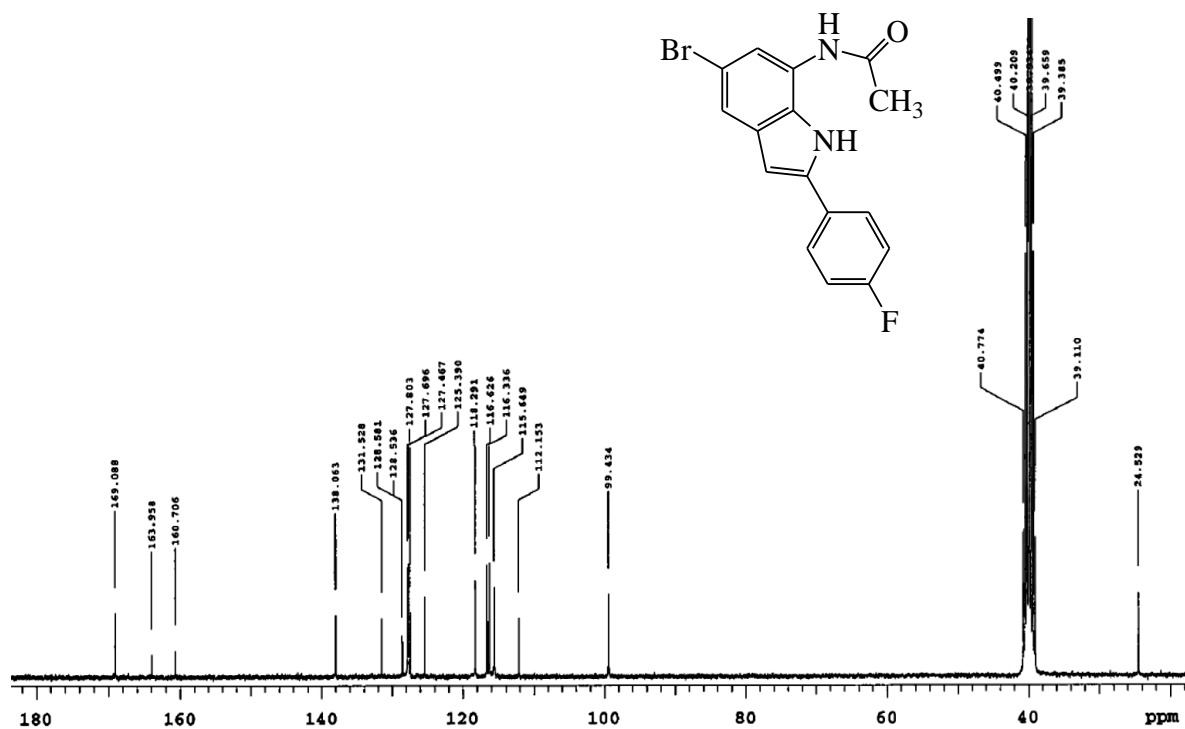
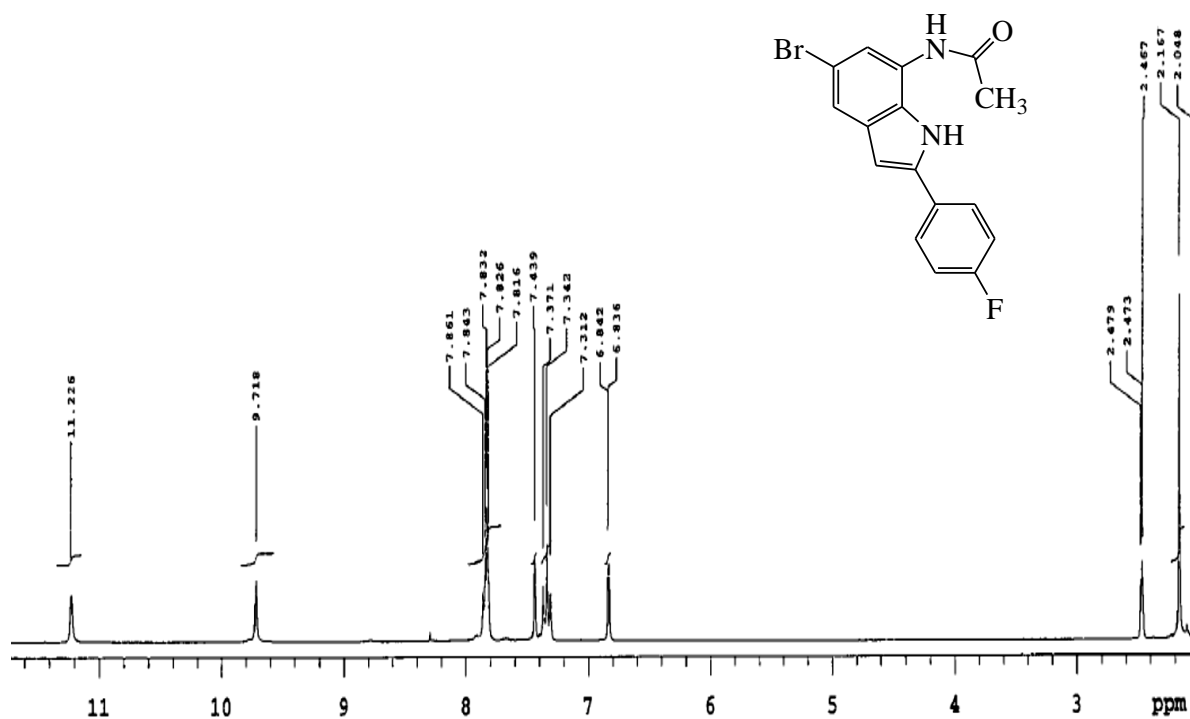


Figure S1.10: <sup>1</sup>H- and <sup>13</sup>C-NMR spectra of **4b** in DMSO-*d*<sub>6</sub> at 300 MHz and 75 MHz, respectively.

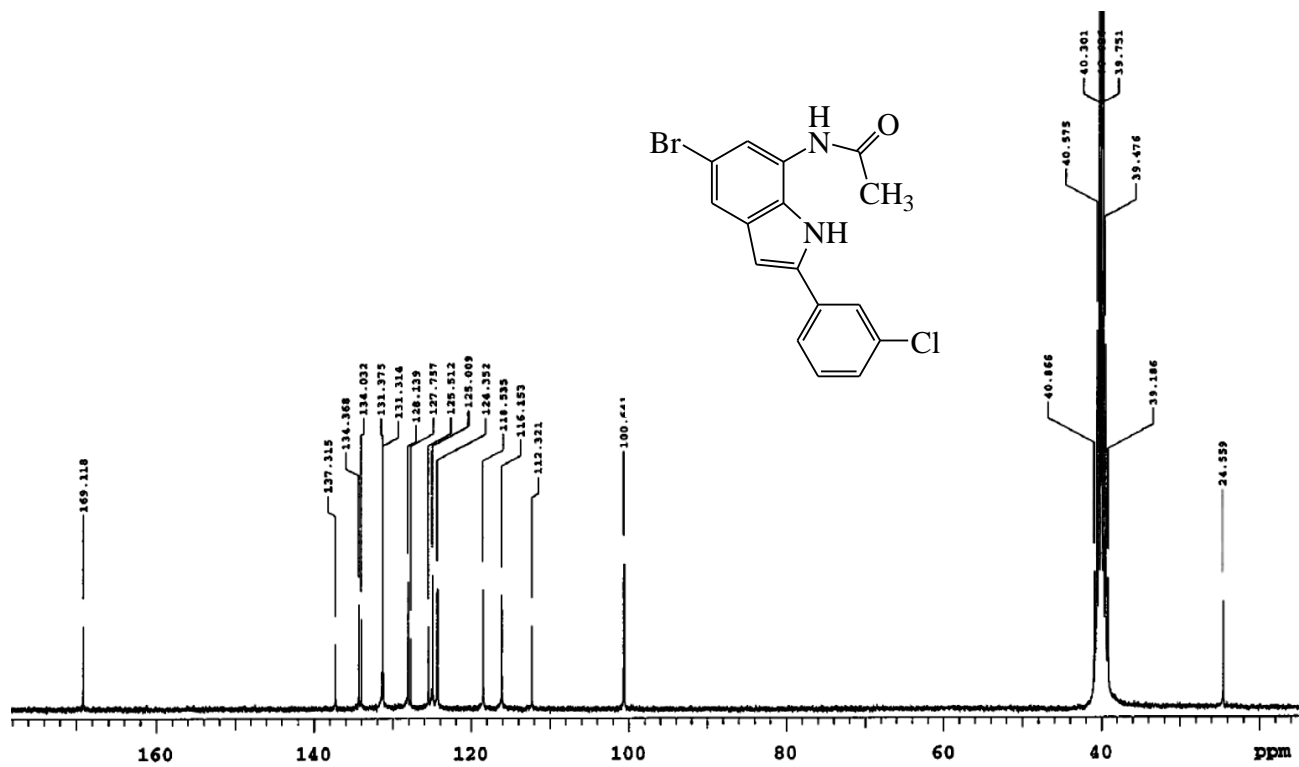
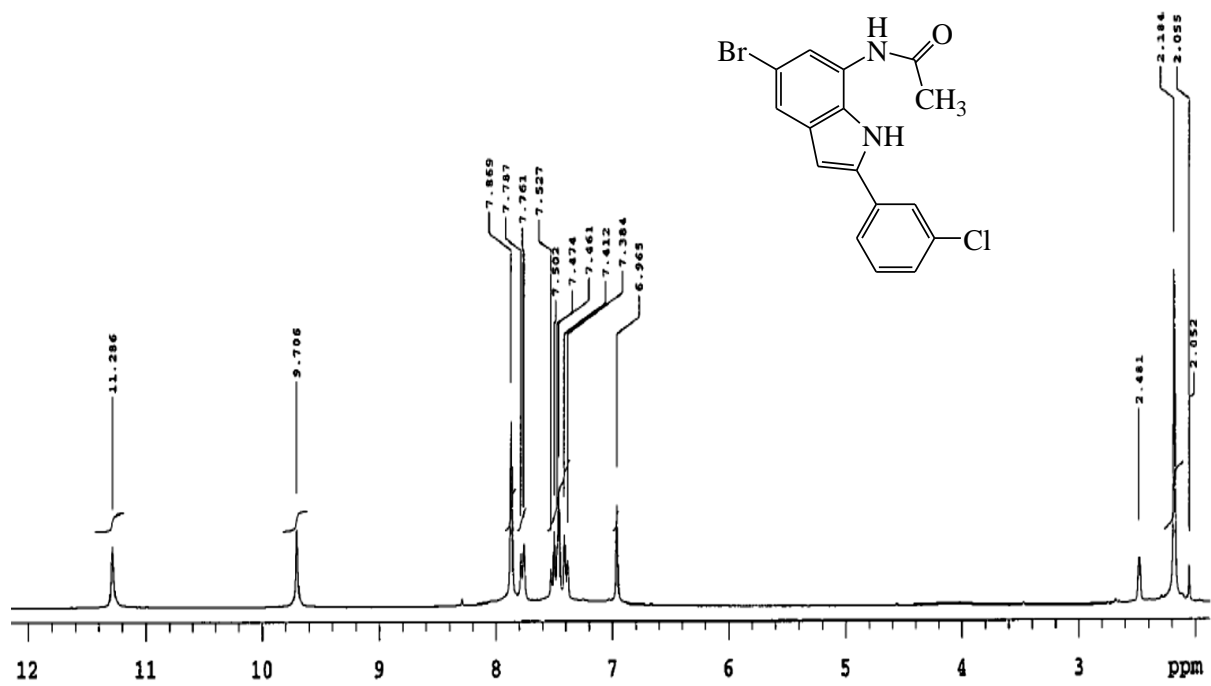


Figure S1.11: <sup>1</sup>H- and <sup>13</sup>C-NMR spectra of 4c in DMSO-*d*<sub>6</sub> at 300 MHz and 75 MHz, respectively.

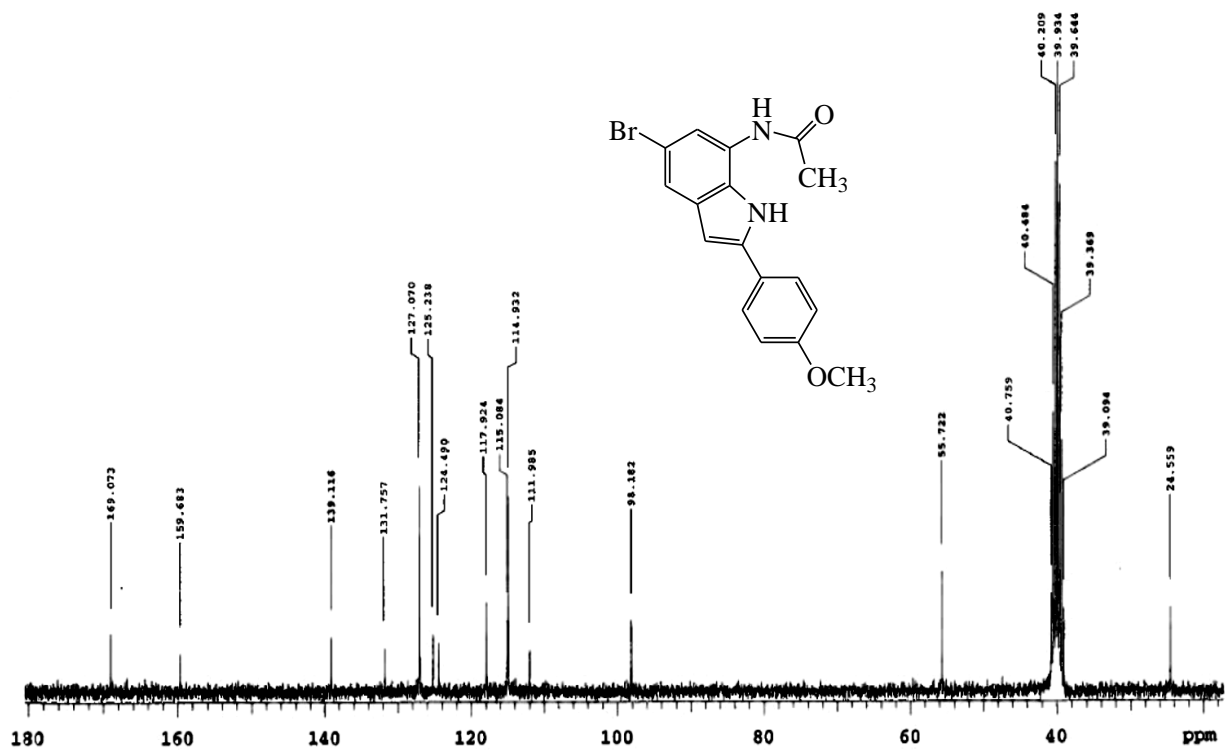
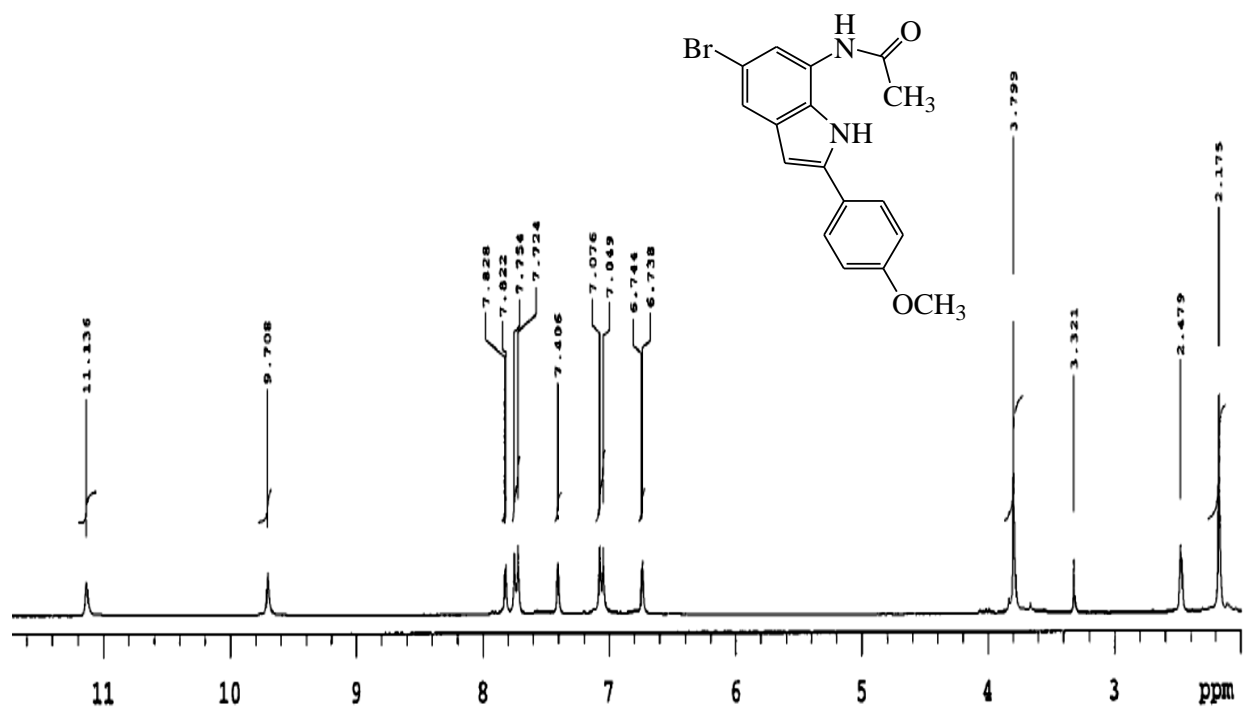


Figure S1.12: <sup>1</sup>H- and <sup>13</sup>C-NMR spectra of 4d in DMSO-*d*<sub>6</sub> at 300 MHz and 75 MHz, respectively.

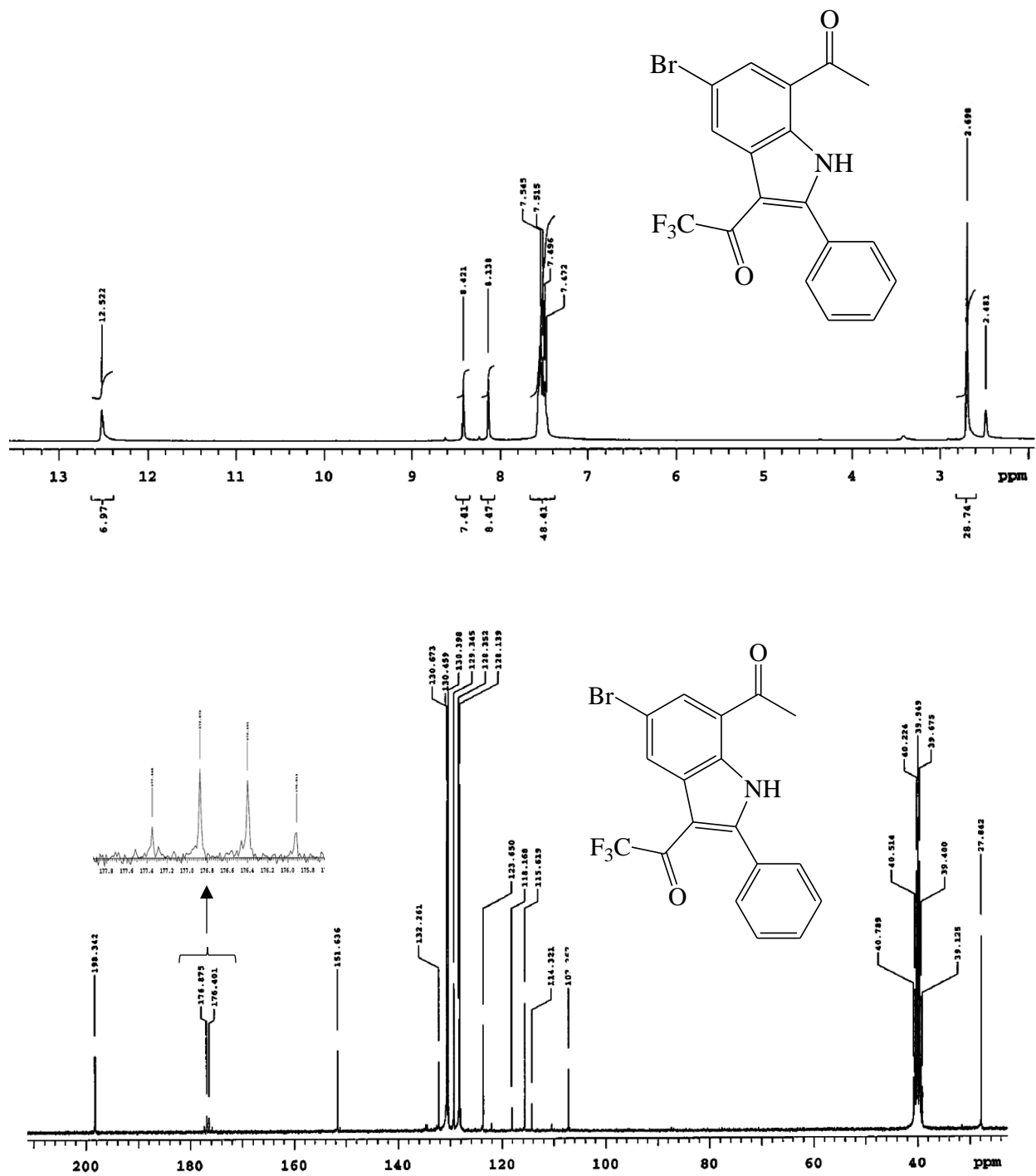


Figure S1.13: <sup>1</sup>H- and <sup>13</sup>C-NMR spectra of 5a in DMSO-*d*<sub>6</sub> at 300 MHz and 75 MHz, respectively.

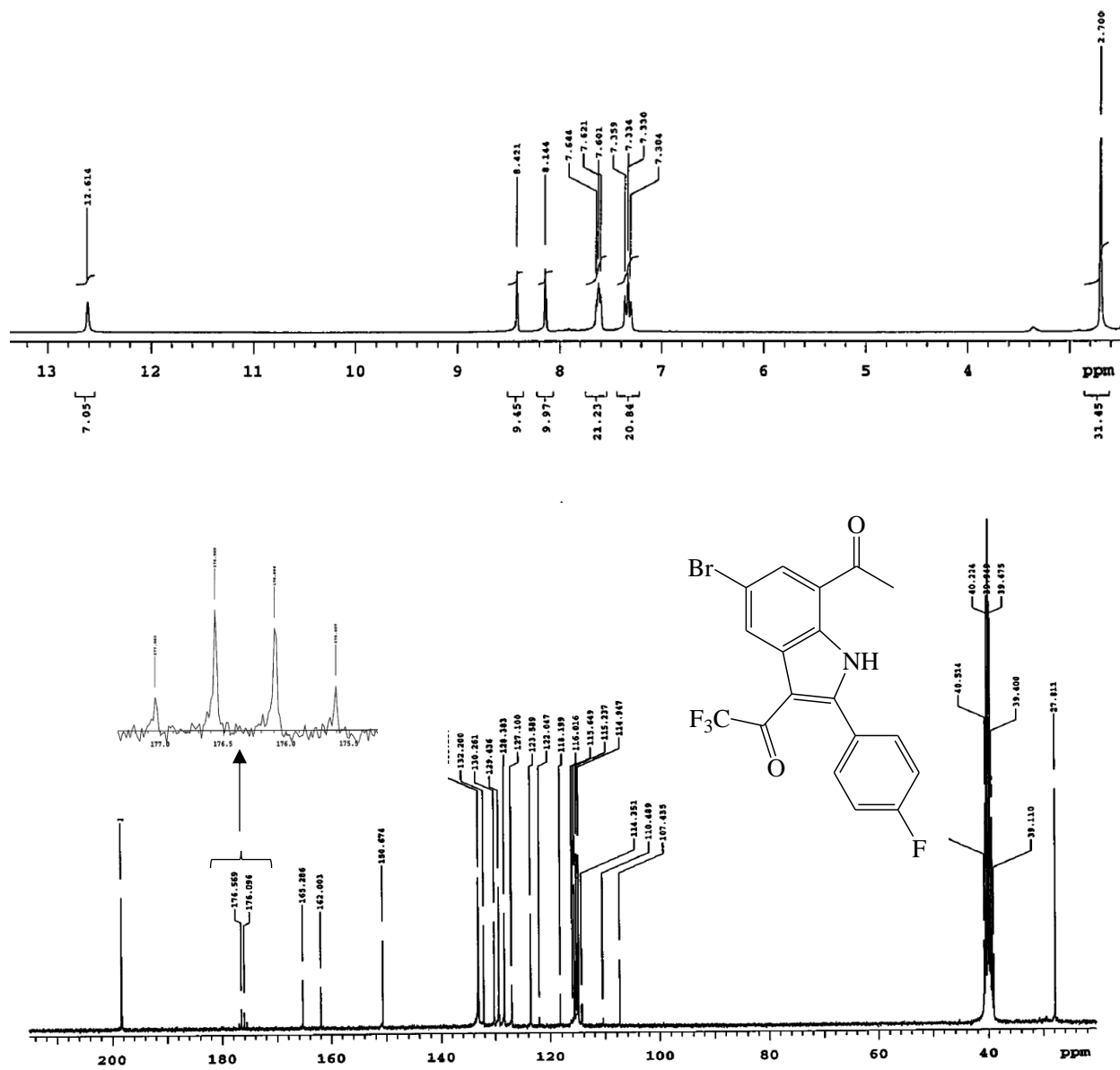


Figure S1.14: <sup>1</sup>H- and <sup>13</sup>C-NMR spectra of 5b in DMSO-*d*<sub>6</sub> at 300 MHz and 75 MHz, respectively.

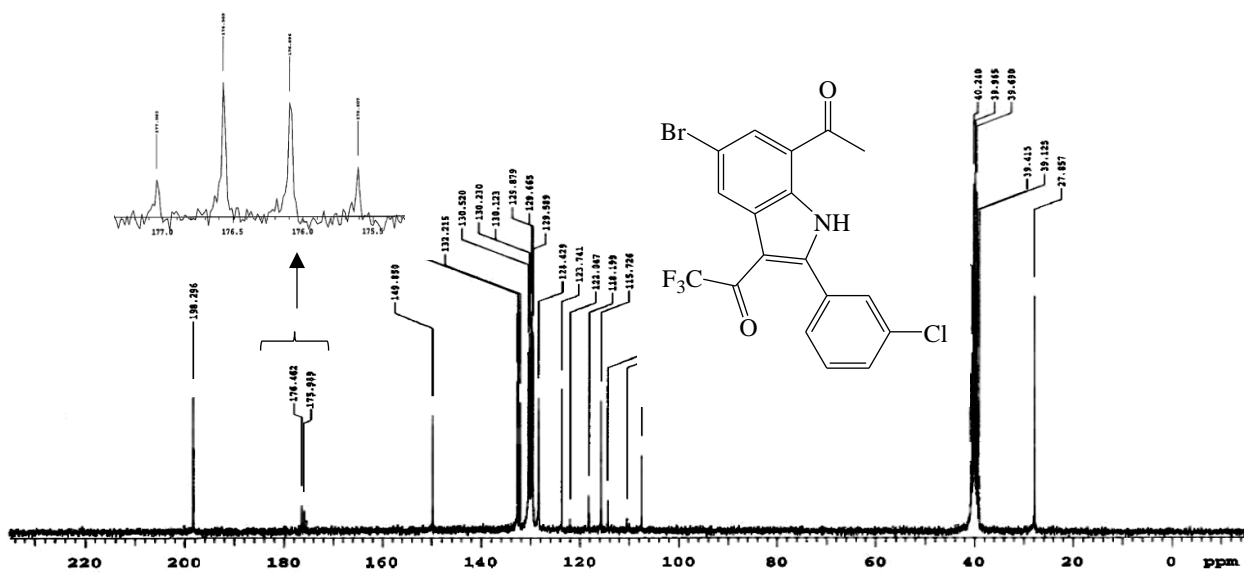
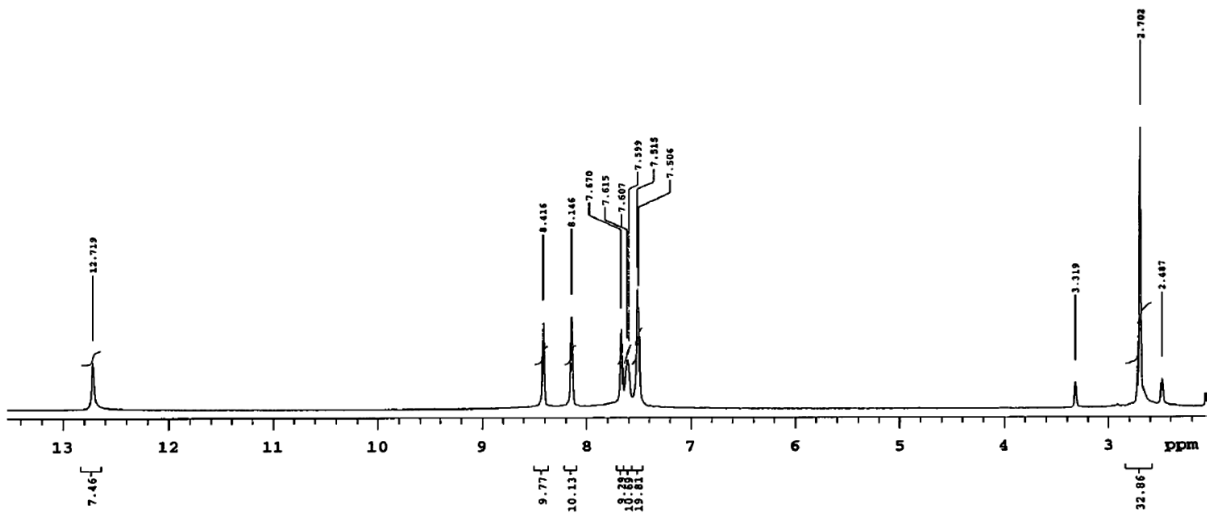


Figure S1.15:  $^1\text{H}$ - and  $^{13}\text{C}$ -NMR spectra of **5c** in  $\text{DMSO-}d_6$  at 300 MHz and 75 MHz, respectively.



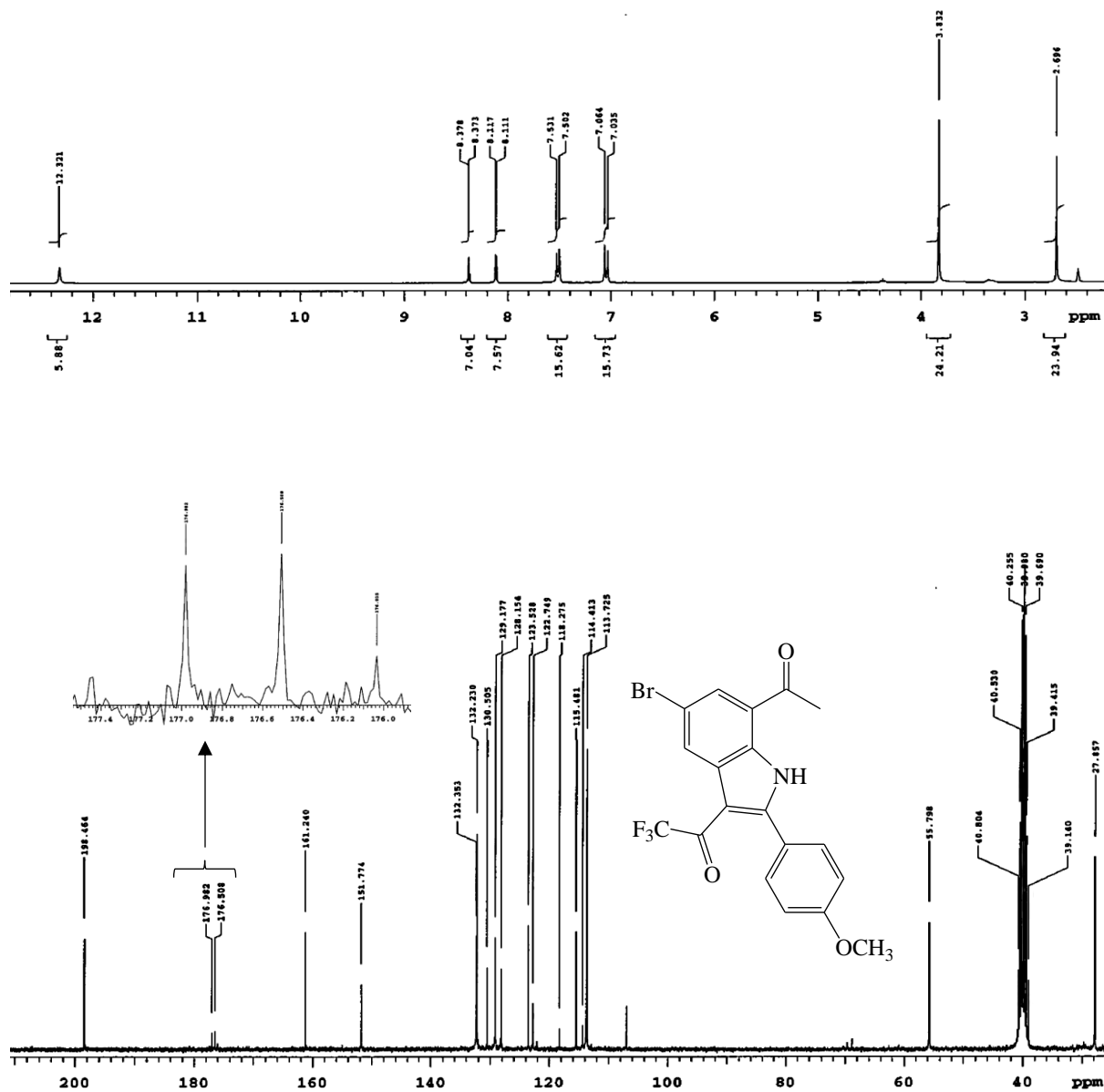


Figure S1.16:  $^1\text{H}$ - and  $^{13}\text{C}$ -NMR spectra of **5d** in  $\text{DMSO-}d_6$  at 300 MHz and 75 MHz, respectively.

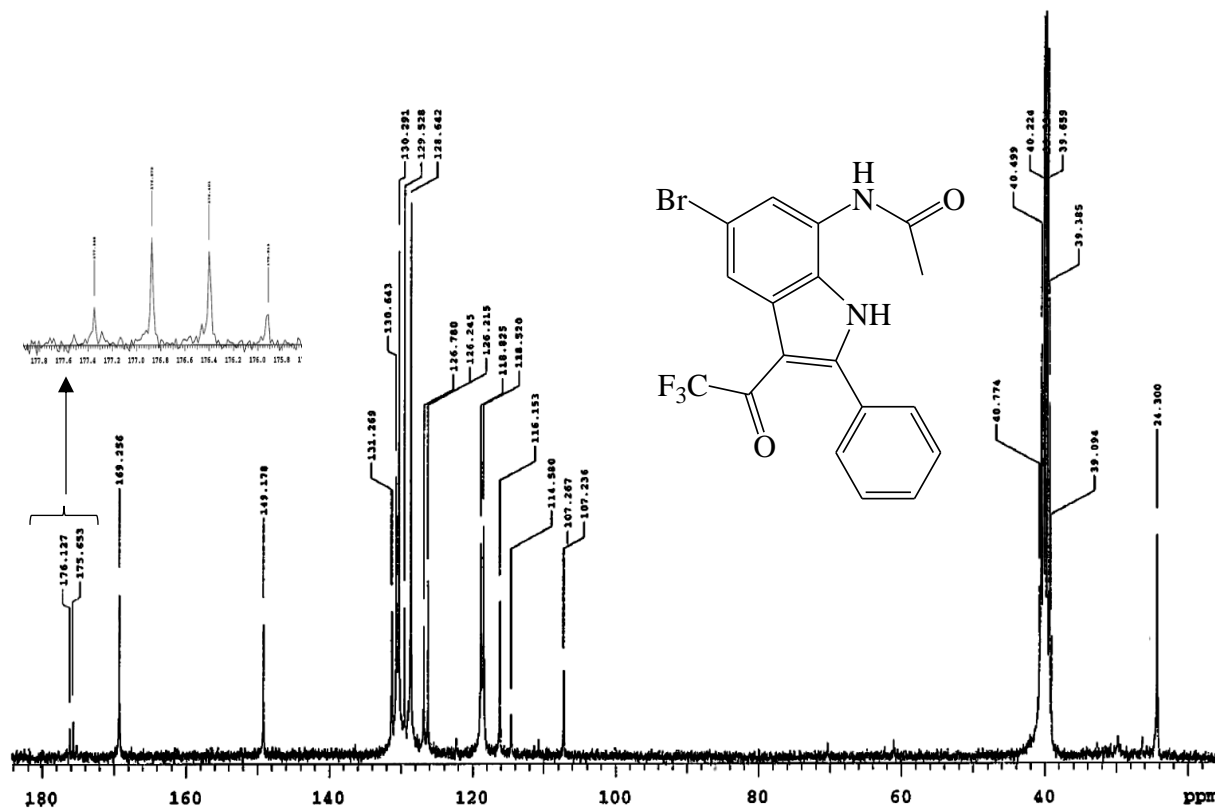
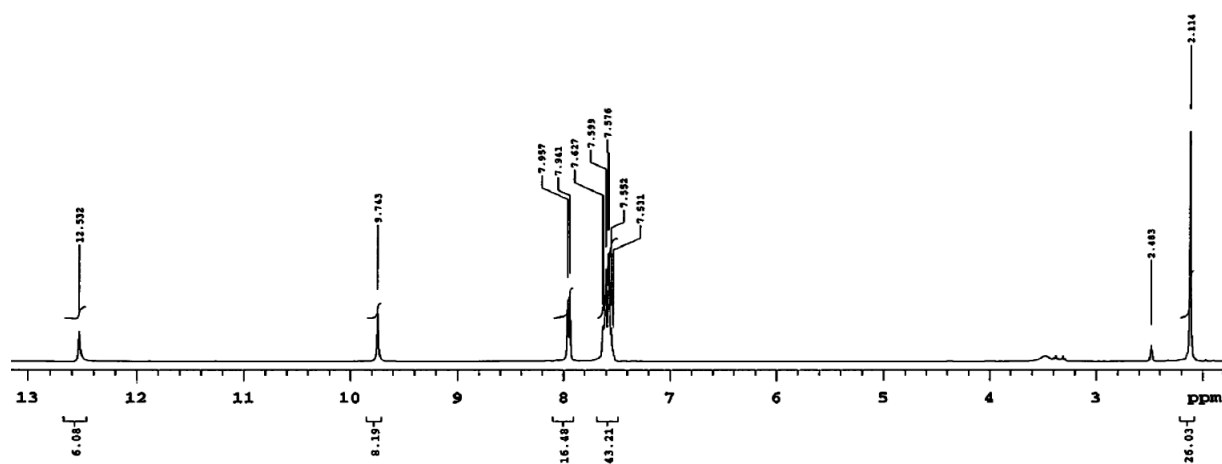


Figure S1.17: <sup>1</sup>H- and <sup>13</sup>C-NMR spectra of 5e in DMSO-*d*<sub>6</sub> at 300 MHz and 75 MHz, respectively.

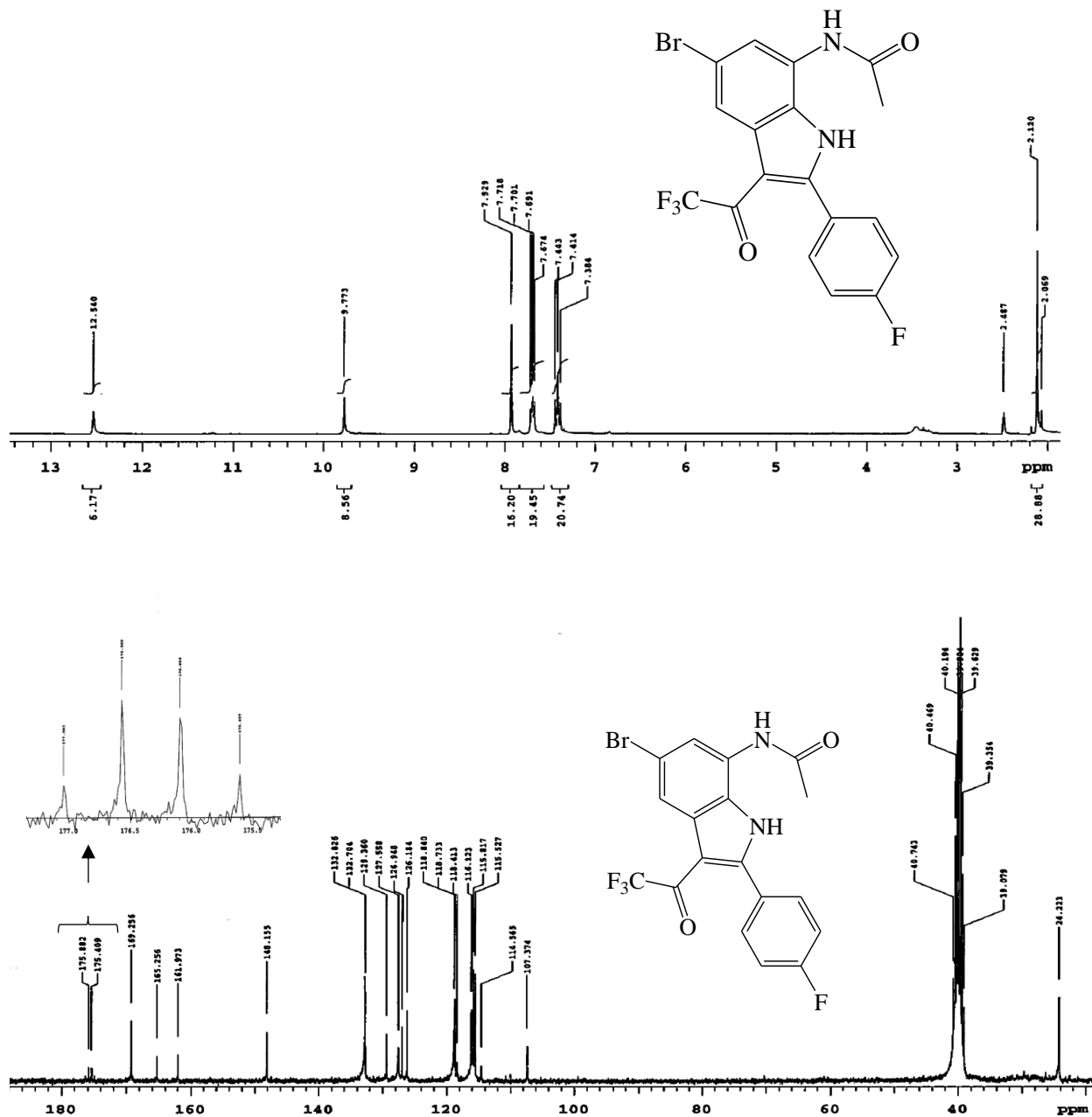


Figure S1.18: <sup>1</sup>H- and <sup>13</sup>C-NMR spectra of 5f in DMSO-*d*<sub>6</sub> at 300 MHz and 75 MHz, respectively.

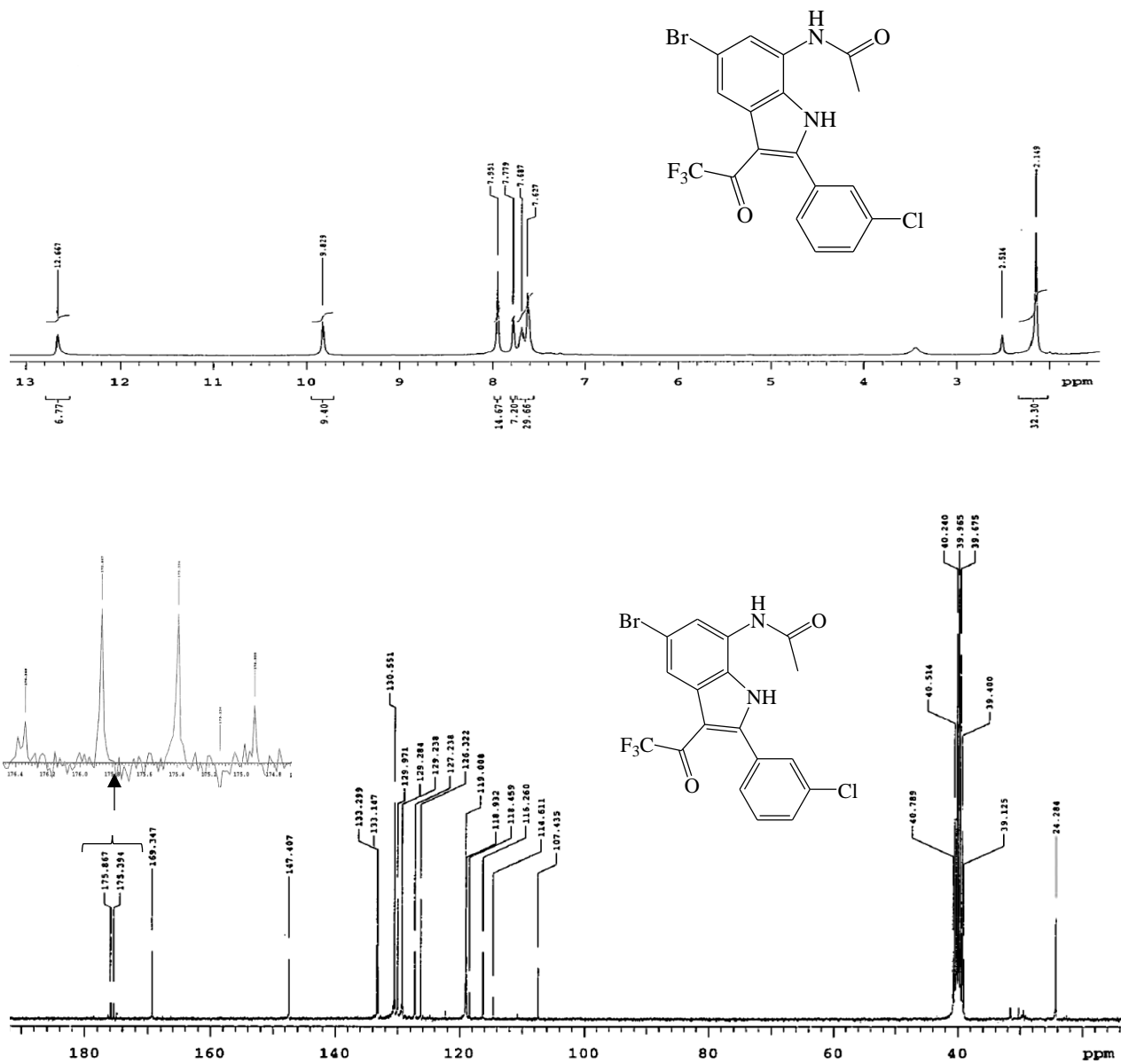


Figure S1.19: <sup>1</sup>H- and <sup>13</sup>C-NMR spectra of 5g in DMSO-*d*<sub>6</sub> at 300 MHz and 75 MHz, respectively.

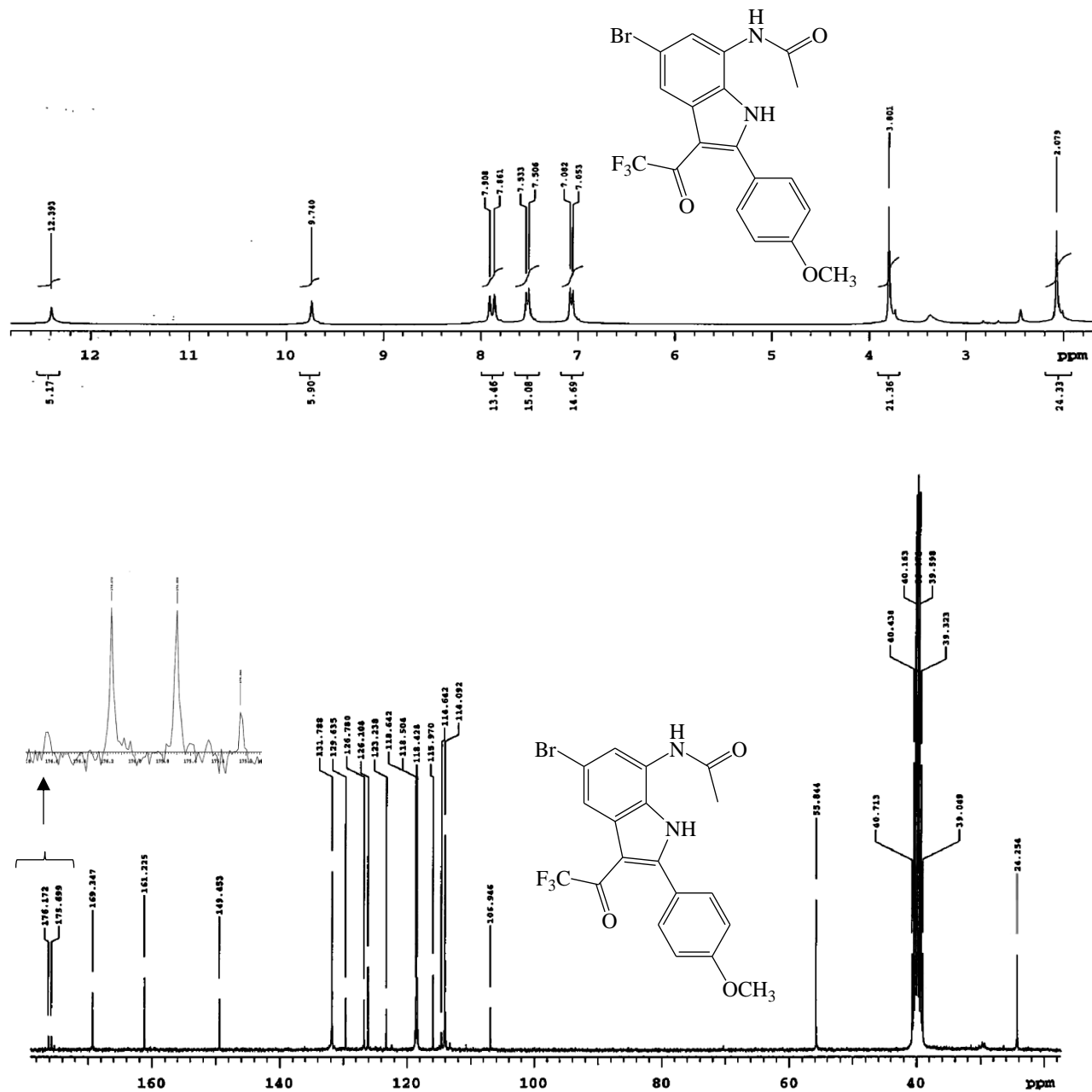
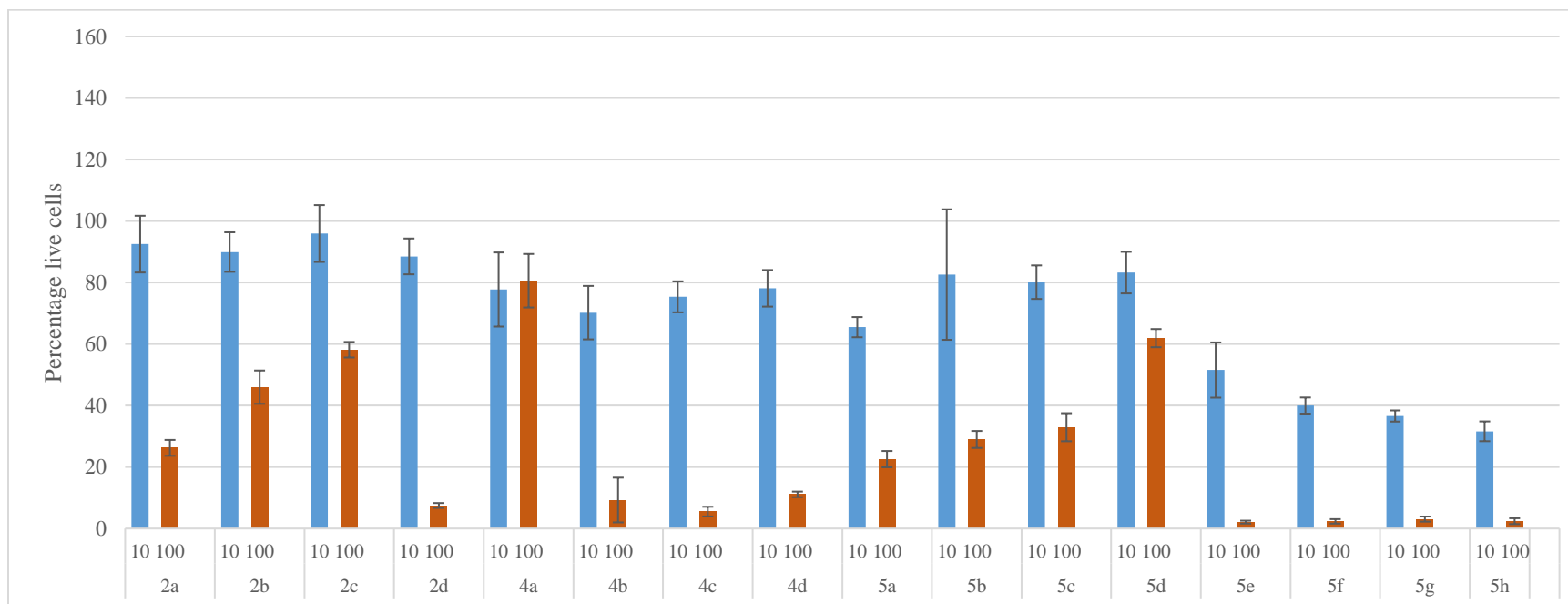
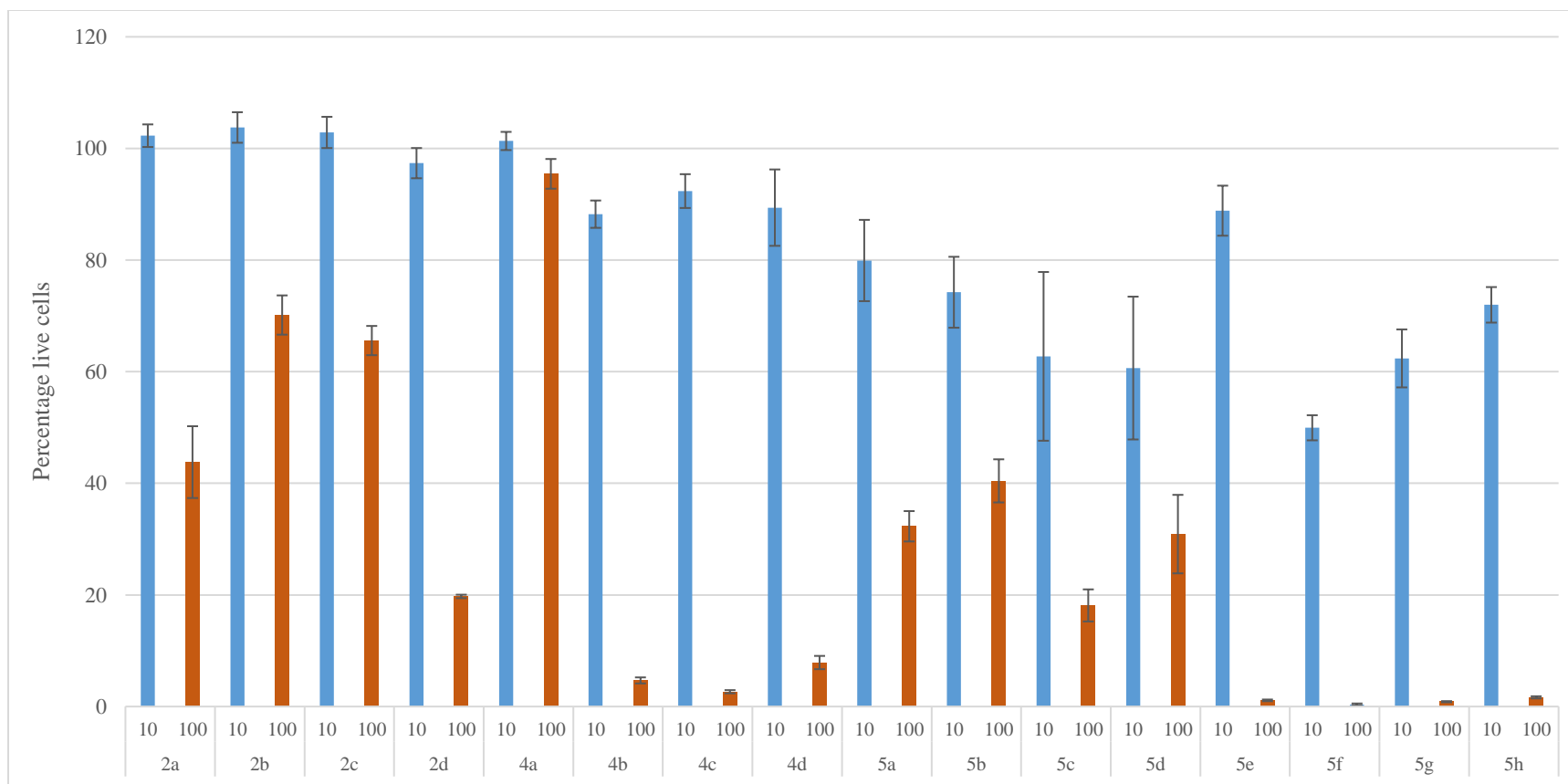


Figure S1.20: <sup>1</sup>H- and <sup>13</sup>C-NMR spectra of 5h in DMSO-*d*<sub>6</sub> at 300 MHz and 75 MHz, respectively.

**Figure S2:** Cytotoxicity of compounds **2a–d**, **4a–d** and **5a–h** against A549 and HeLa cells



**Figure S2.1:** Cytotoxicity of **2a–d**, **4a–d** and **5a–h** at 10  $\mu$ M (blue bar) and 100  $\mu$ M (orange bar) against A549 cells. The results are indicated as percentage live cells compared to an untreated control. Error bars denote standard deviation of one experiment performed in quadruplicate.



**Figure S2.2:** Cytotoxicity of **2a–d**, **4a–d** and **5a–h** at 10  $\mu\text{M}$  (blue bar) and 100  $\mu\text{M}$  (orange bar) against HeLa cervical cancer cells. The results are indicated as percentage live cells compared to an untreated control. Error bars denote standard deviation of one experiment performed in quadruplicate.

Figure S3: Dose response curves for 5e-h against the A549 and HeLa cells

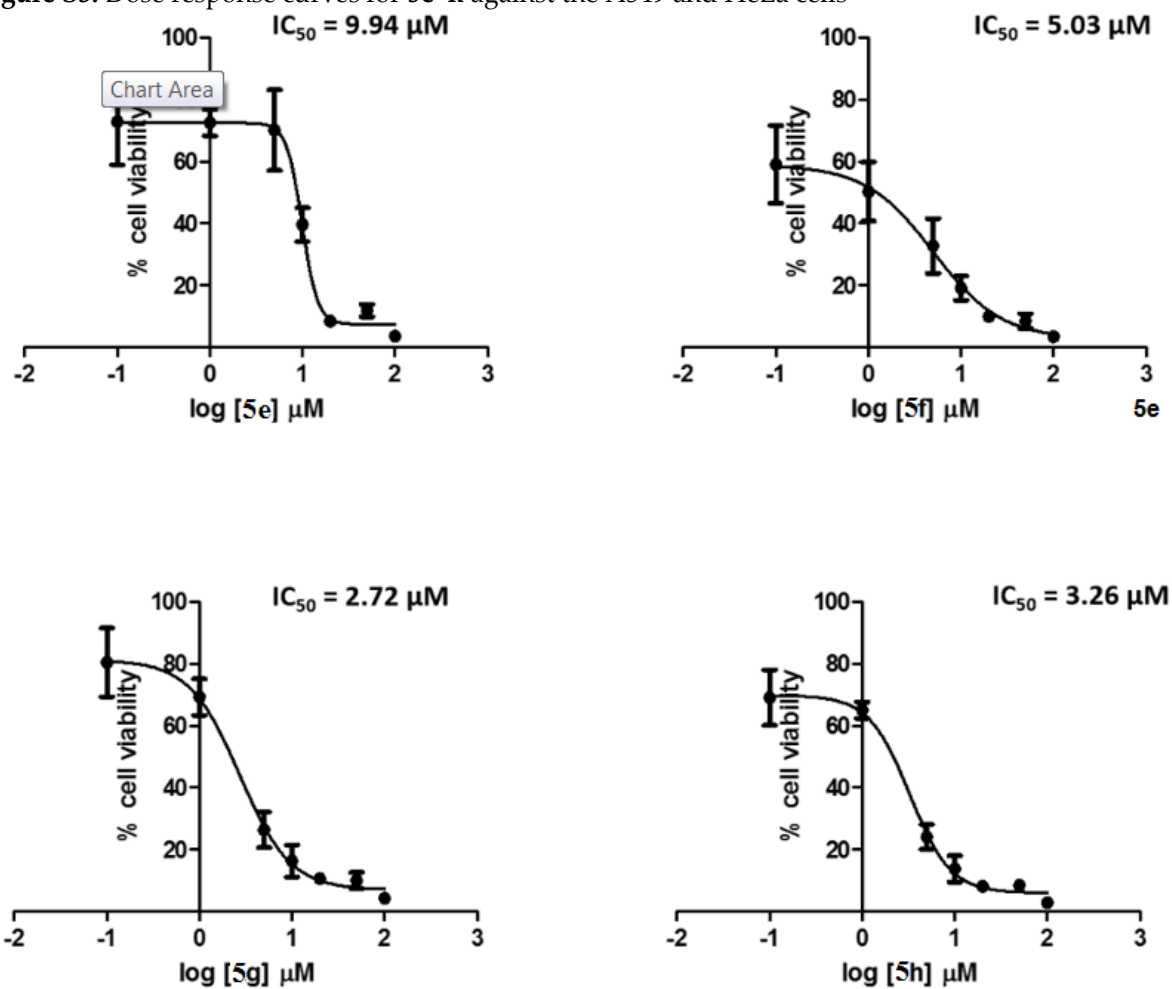
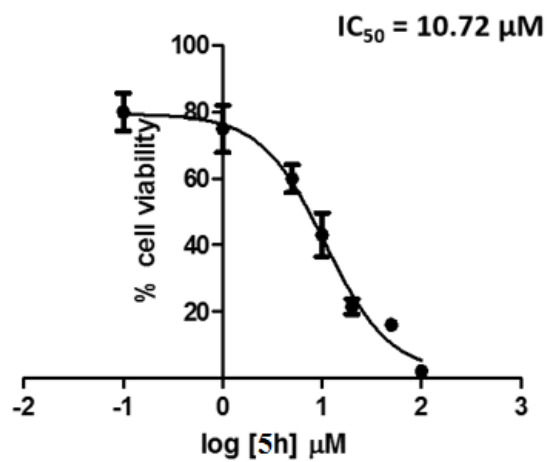
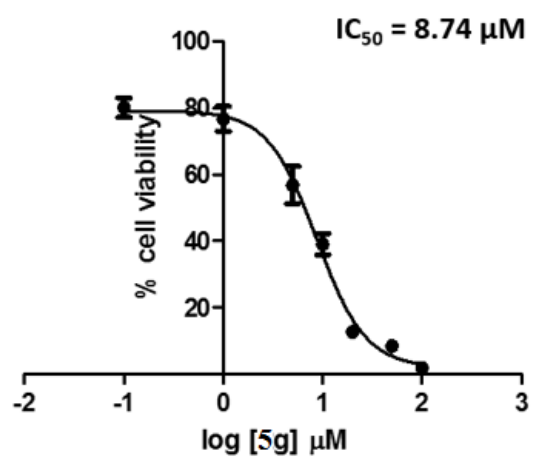
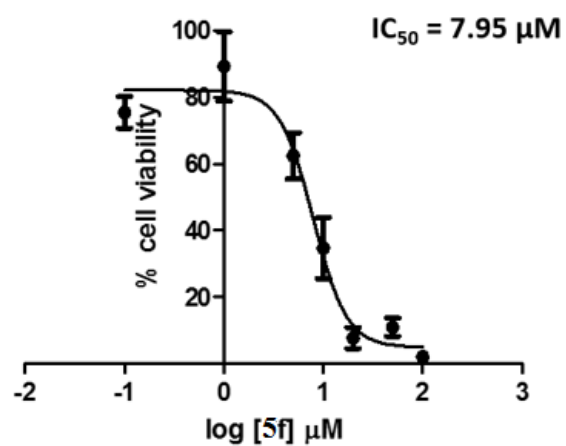
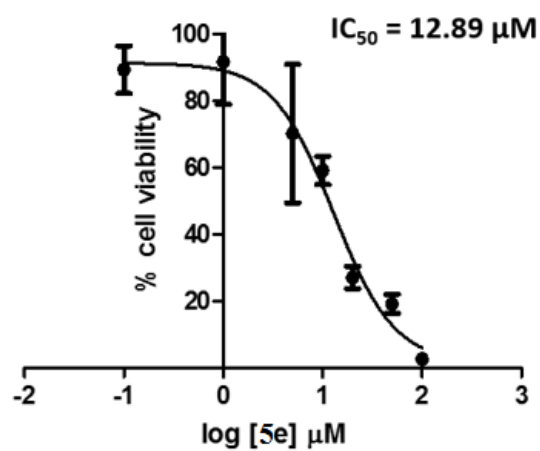


Figure S3.1: Dose response curves for compounds 5e-h against A549 lung cancer cells. Data represents the mean  $\pm$  SD for six replicate wells at each of the indicated concentrations.





**Figure 3.2:** Dose response curves for 5e–h against HeLa cells. Data represents the mean  $\pm$  SD for six replicate wells at each of the indicated concentrations.

**Figure S4:** Spread sheet for statistical analysis which contains p values for each test



Copy of processed  
results\_screening of c



Copy of processed  
results\_screening of c

**Figure S5:** Excel spreadsheets for raw data and SD values for compounds **5e–h** as well as GraphPad Prism files for IC<sub>50</sub> determination



RE SD and raw  
data.msg